J Solid State Electrochem (2011) 15:2489–2522
DOI 10.1007/s10008-011-1506-5

REVIEW

The method of limited volume electrodes as a tool for hydrogen electrosorption studies in palladium and its alloys

Mariusz Łukaszewski · Andrzej Czerwiński

Received: 4 May 2011 / Revised: 30 June 2011 / Accepted: 3 July 2011 / Published online: 17 August 2011

Abstract The review summarizes selected aspects of the electrochemical investigations on hydrogen absorption in palladium and its alloys prepared as thin layers deposited on a conductive substrate. These kinds of electrodes are named "limited volume electrodes" (LVEs). We demonstrate that LVE methodology creates new possibilities for electrochemical studies on hydrogen-absorbing materials. In this paper, we describe the procedures of preparation and characterization of Pd-based LVEs and give a survey of the investigations on hydrogen electrosorption performed with the use of LVEs. We discuss the influence of such factors as electrode potential, temperature, electrolyte composition, electrode thickness, and other experimental conditions on the process of hydrogen and deuterium absorption in Pd LVEs. The results concerning Pd alloys are thoroughly reviewed. The studies on thermodynamics, kinetics, and mechanism of hydrogen electrosorption in Pd and its alloys are also summarized. Attention is paid to the examination of the interrelation between hydrogen absorption and other electrochemical processes taking place on LVEs. Finally, possible applications of the LVE methodology in the context of electrochemical power sources are mentioned.

Keywords Palladium · Palladium alloys · Hydrogen absorption · Limited volume electrodes (LVEs) · Thin layers

Introduction

It has been known for almost 150 years that many transition metals can react with hydrogen forming non-stoichiometric hydrides in which hydrogen occupies interstitial voids in metal crystal lattice [1–9]. Since that time, hydrogen–metal systems have found important applications as catalysts in hydrogenation reactions, reacting substances in the synthesis of transition metal alloys, neutron moderators in nuclear power engineering, and getters in vacuum systems [9]. Metal hydrides can also be utilized as membranes for hydrogen purification and hydrogen isotope separation or as a source of hydrogen of high purity by thermal decomposition of hydrides [9–11]. Highly pure hydrogen is widely used in the electronics, metallurgy, as well as fine chemistry, food, and drug industries.

Due to the fact that hydrogen is now regarded as a promising energy carrier, interest in hydrogen–metal systems has been growing continuously in recent years. Hydrogen is very attractive as it has high-energy, is easily available, and is non-toxic fuel, but the large volume of hydrogen containers and the danger of explosion connected with its storage in gas or liquid phase are two of the main barriers against hydrogen use on a large scale. For economic and safety reasons, hydrogen storage in metal hydrides seems to be much more convenient [12–14].

Hydrogen–metal systems are also important in electrochemical power sources. Metal alloys saturated with hydrogen are utilized as the anodes in commonly used rechargeable nickel–hydride batteries (Ni–MH), which have many advantages over lead–acid and nickel–cadmium batteries [15, 16]. Hydrogen–metal systems can also be used as the source of hydrogen in fuel cells. Recently, the possibility of the use of hydrogen–metal systems in supercapacitors has been demonstrated [17–20].

Since its early discovery by Graham in 1866, the palladium–hydrogen system has been playing a particularly important role among other metal–hydrogen systems [3, 6].

M. Łukaszewski · A. Czerwiński (✉)
Department of Chemistry, Warsaw University,
Pasteura 1,
02-093 Warsaw, Poland
e-mail: aczerw@chem.uw.edu.pl

Despite limited practical use due to high cost and great atomic mass of Pd, it has been widely studied as a model system for this class of materials. By investigating Pd behavior in the process of hydrogen absorption and the influence of Pd alloying with other metals on their absorption properties, we can understand better the complex reactions taking place in multi-component alloys designed for hydrogen storage or used as electrodes in rechargeable hydride batteries [16]. By examining the influence of other metal additives to Pd on the absorption behavior, it is possible to understand the role of various factors such as the structural, electronic, or elastic properties of the alloy on its ability to absorb hydrogen. Thus, studies on the chemical and electrochemical properties of Pd and its alloys are important both from the fundamental and the practical points of view.

In our paper, we summarize the results of the electrochemical studies on hydrogen absorption in Pd and Pd alloys. Since this topic is very wide and it would be extremely difficult to cover all the possible aspects of the above phenomenon, we decided to focus on the electrochemical investigations performed with the use of thin Pd films (with a thickness of the order of micrometers) deposited on a hydrogen-neutral matrix. This kind of electrode has been named "limited volume electrode" (LVE). For general information on the properties of metal-hydrogen and palladium–hydrogen systems, we refer the reader to the literature [1–7, 9, 21]. A survey of the results of the investigations on hydride batteries is presented in [16, 22–28]. Detailed information on the progress in research on hydrogen storage materials can be found in [29–39]. Various aspects of hydrogen energy are discussed in [12–14, 40]. A comprehensive reference to books, bibliographies, workshops, and conferences on hydrogen in metals and other materials is given in [41]. A detailed discussion on Pd electrochemistry in the aspect of surface oxidation/metal dissolution is given elsewhere [42–57]. In the literature, there are numerous reports devoted to electrocatalysis on Pd-based electrode materials, e.g., on the oxidation of carbon monoxide [58–69], methanol [60, 70–74], ethanol [74–80], and formic acid/formates [81–98] and the reduction of oxygen [99–111] or hydrogen oxidation/evolution [112–114]. Our review will be limited to certain points connected with hydrogen-related phenomena. Other aspects of Pd electrochemistry have been summarized in an earlier paper [115].

General characteristic of hydrogen sorption in Pd

Hydrogen sorption in Pd, as in many other metals/alloys, can be realized directly from the gas phase [1–3], i.e., by metal exposure to gaseous hydrogen under a given pressure or electrochemically, i.e., by hydrogen generation from a protonic electrolyte, after the application of a suitable potential value to a metallic electrode [16, 47]. It is also possible to perform hydrogen absorption in Pd from electrolytes saturated with gaseous hydrogen [116–118]. In the next sections, we will focus on electrochemical absorption.

Even at room temperature, Pd easily absorbs large amounts of hydrogen, forming a non-stoichiometric compound, PdH_x. Since the phase diagram of the Pd–H system is characterized by a miscibility gap, hydrogen absorbed in Pd can exist in two separate phases [3, 119–123]. For a small amount of hydrogen, the α-phase appears, which can be treated as an ideal dilute solid solution of hydrogen in Pd. At room temperature, the atomic ratio between hydrogen and Pd (H/Pd) in the α-phase is below approx. 0.03–0.05 [3, 45, 124, 125]. When the amount of hydrogen increases, the β-phase starts forming, described as Pd hydride, for which the model of ideal dilute solution cannot be applied. At room temperature, the minimum composition of the pure β-phase corresponds to a H/Pd ratio approx. 0.6 [3, 45, 124, 125]. Under normal conditions, when Pd is in equilibrium with gaseous hydrogen, the H/Pd ratio is 0.69 [45]. A similar value (0.73) is obtained for a Pd electrode polarized at a potential slightly higher than the hydrogen evolution potential [126–128]. Under normal conditions, the volume of hydrogen gas absorbed is even 950 times greater than the volume of a Pd specimen itself. With the increase in temperature, the maximum concentration of hydrogen in the α-phase increases, while the minimum concentration of hydrogen in the β-phase decreases. At the critical point of the Pd–H system (temperature approx. 570 K, pressure approx. 20 atm), the parameters of both phases become identical (H/Pd≈0.25–0.30) and the miscibility gap disappears [3, 119–123].

It was established using the methods of neutron diffraction and NMR that hydrogen is present inside Pd not in the molecular form but most probably in the form of protons, which occupy octahedral voids in the Pd crystal lattice of a face-centered cubic (fcc) type [3, 119–123], while the electrons from the H atoms are transferred to the Pd d band, filling the empty states. In the presence of absorbed hydrogen, the Pd crystal lattice expands, the unit cell dimensions increase, only slightly for the α-phase (from 0.3890 nm to approx. 0.3895 nm) and significantly (above 0.4025 nm, i.e., by more than 3% in comparison with pure Pd) for the β-phase [124, 125]. The expansion of the crystal lattice leads to stresses accompanying hydrogen absorption in metals and alloys [53, 55, 129–157]. However, the fcc type of Pd crystal lattice is retained during hydrogen absorption. The interactions with hydrogen result also in changes in the other physical properties of

Pd, such as magnetic susceptibility, electrical resistance, or elastic properties [3, 119–123, 158–170].

Besides the ability to absorb hydrogen, Pd, as other platinum group metals, can also adsorb hydrogen [45, 47]. In electrochemical experiments, the potential region of hydrogen adsorption is overlapped with that of hydrogen absorption, and the separation of both these processes requires special procedures. The contribution of adsorbed hydrogen to the total amount of electrosorbed hydrogen becomes important only for very thin or rough Pd layers.

According to a model presented by Jerkiewicz and Zolfaghari [47, 171], hydrogen adsorbed on Pd, as well on Pt, Ir, and Rh, can occupy two different sites on the surface, namely, a hollow site or an on-top position. The former state is related to underpotentially deposited hydrogen (UPD H), while the latter concerns overpotentially deposited hydrogen (OPD H). UPD H appears on the Pd surface at potentials considerably higher than the hydrogen evolution potential and does not participate in hydrogen evolution reaction. On the other hand, OPD H is the only form involved in the hydrogen evolution process. Both these forms may be the source of absorbed hydrogen.

Idea of LVEs

Electrochemical hydrogen insertion into Pd has commonly been applied in absorption studies since the pioneer work by Graham [3]. Pd is especially attractive and convenient for electrochemical experiments due to the fact that hydrogen absorption can be realized at room temperature without corrosion of the electrode material [16]. However, one of the important problems in studying hydrogen electrosorption process in Pd and Pd alloys in the form of wires or foils is the generation of absorption/desorption currents, which are a few orders of magnitude higher than those originating from surface processes. Figure 1 presents a cyclic voltammogram recorded over a wide potential range (−0.10 to 1.50 V vs. the reversible hydrogen electrode, RHE) for a bulk Pd electrode (a wire of 1-mm diameter). In that case, in the hydrogen electrosorption region, a monotonic increase in cathodic current is observed below 0.10 V (region A in Fig. 1), followed in the anodic scan by a broad peak at approx. 0.20–0.30 V (region B). Because of diffusional limitations, the oxidation of a large amount of hydrogen dissolved in the metal occurs slowly, which results in the domination of hydrogen oxidation signals over surface oxidation currents (above 0.70 V, region C). Hydrogen desorption still proceeds even after reversing polarization, which is mirrored in the fact that during a cathodic scan within the oxygen region a resultant positive current is observed (see insert in Fig. 1), even in the region of the surface oxide reduction peak (signal D at 0.70 V). Therefore, using bulk Pd samples, it is very

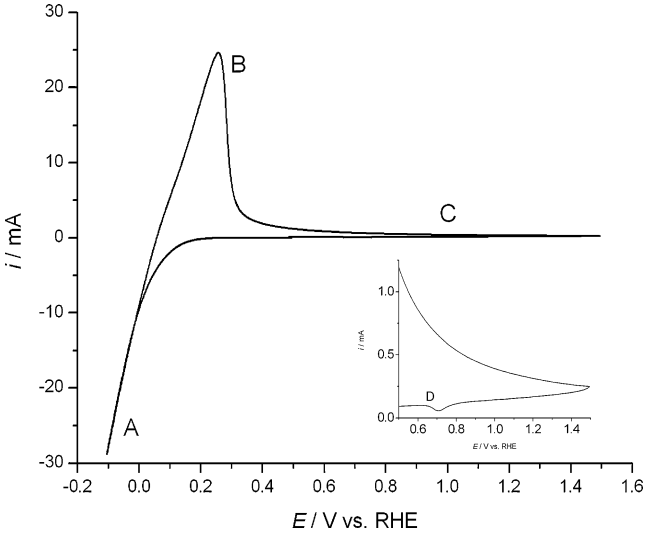

Fig. 1 Cyclic voltammograms (0.02 Vs^{-1}) for a Pd wire (diameter, 1 mm) in acidic solution (0.5 M H_2SO_4) at room temperature. *Insert* shows the oxygen region

difficult to study electrochemically the process of hydrogen absorption and to separate the electrochemical response originating from that process and the contributions from other reactions that can simultaneously take place on the electrode surface.

The above problem has been eliminated by the use of a thin Pd layer deposited on a conductive, hydrogen-neutral matrix. Such an approach allows for the limitation and control of the amount of sorbed hydrogen. In cyclic voltammetric experiments performed with this kind of electrode, hydrogen oxidation peaks can be easily separated from the currents of various surface reactions. Figure 2a shows a cyclic voltammogram (CV) for a thin Pd layer (0.8 μm thick) recorded under the same experimental conditions as for a Pd bulk electrode in Fig. 1. It is clearly demonstrated that in the latter case, hydrogen can be absorbed and then totally be oxidized in a narrow potential range during a single CV scan. Already above 0.20 V vs. RHE, the current drops to the value connected with double-layer charging and further surface oxidation (signal C in Fig. 2a). Thus, the use of a thin Pd deposit results in hydrogen absorption/desorption signals and surface oxidation/oxide reduction currents of a comparable magnitude and well separated from each other. In particular, the surface oxide reduction peak (*D*) is well defined and appears without a significant background, as observed for a Pd wire. From the charge under this peak, the real surface area of the Pd electrode can be determined [45, 172].

First attempts to use a thin Pd-based layer in electrochemical studies were done by Tverovskii and Vert et al. [21]. Woods [173] electrodeposited thin Pd–Au alloys on a Au matrix and characterized their electrochemical behavior by cyclic voltammetry in a wide hydrogen–oxygen poten-

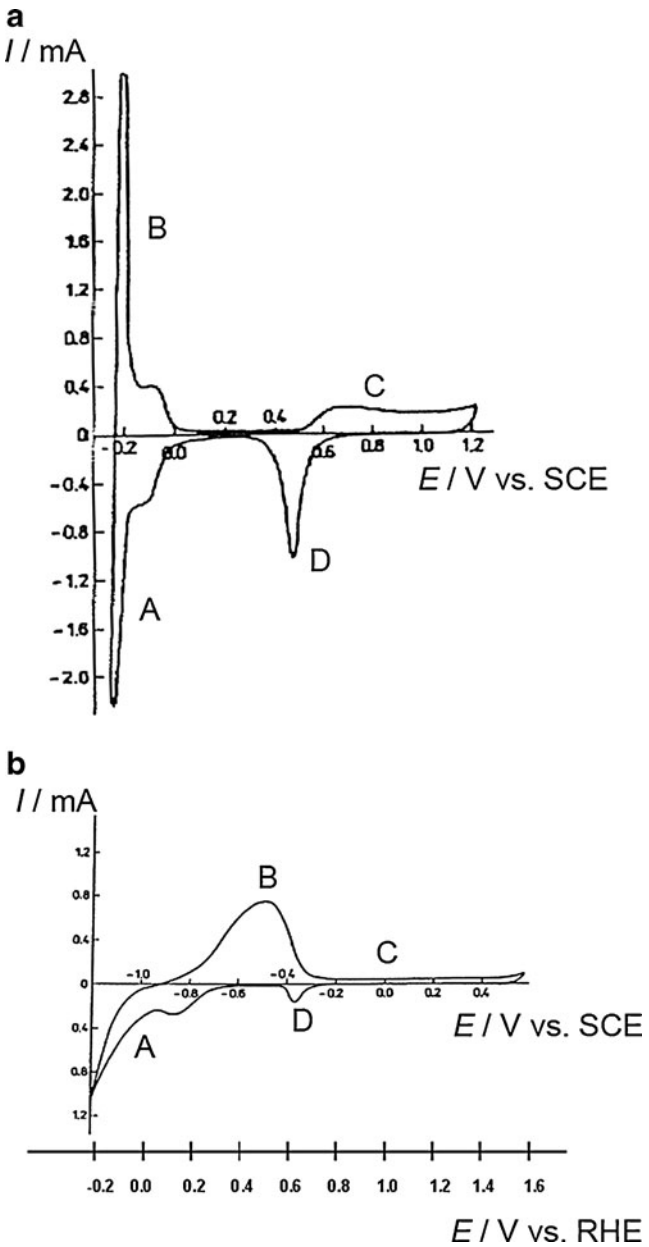

Fig. 2 Cyclic voltammograms for a Pd LVE (thickness, 0.8 μm) in acidic solution (0.5 M H_2SO_4) (**a**) and basic solution (0.1 LiOH) (**b**) [128] at room temperature. Scan rate: **a** 0.02 Vs^{-1}, **b** 0.01 Vs^{-1}

tial range. Rand and Woods [174] as well as Cadle [175] electrodeposited ultrathin Pd layers on Au, but these studies were limited to the potential region of surface oxidation. Bucur and Stoicovici [176] and Bucur et al. [177] examined hydrogen solubility and absorption mechanism in electrodeposited Pd films (0.26–1 μm) on Pt and quartz support, respectively. Chevillot et al. [178] studied electrochemical hydrogen interactions with Pd electrodes prepared by metal deposition on Au. In the course of cyclic voltammograms recorded in a wide potential region, they could distinguish signals due to hydrogen adsorption and absorption, including two distinct states of adsorbed hydrogen (i.e., more and less strongly bonded to the surface). Frazier and Glosser [179] applied thin Pd layers (6–120 nm) for studying the effect of film thickness on hydrogen absorption in Pd from the gas phase. Thin Pd films were also utilized by Bucur and Flanagan [145], and Bucur and Mecea [180] for quartz crystal microbalance studies on hydrogen absorption in Pd. Horkans [181], using Pd thin films (50–1,000 nm) evaporated on Nb-coated glass, investigated the influence of film thickness on hydrogen electrosorption in Pd, while Nicolas et al. [182, 183] studied the effect of temperature and absorption/desorption cycling for ultrathin (below 60 nm) Pd and Pd–Ag films deposited in vacuum on glass substrate. Thin Pd electrodeposits on Au were also utilized by Gossner and Mizera [184], but their experiments were not related to the hydrogen sorption phenomena. Harris [185] deposited Pd films (2–16 nm) on Si and Ti/Si supports and tested their electrochemical behavior, presenting cycling voltammograms with the hydrogen and oxygen regions well separated from each other, with a well-pronounced fine structure of hydrogen electrosorption signals.

A significant interest in hydrogen electrosorption in Pd rose again in the early 1990s. In 1991, Rosamilia et al. [186] reported on electrochemical hydrogen insertion into Pd and Pd–Ni thin films (1–10 μm) electroplated on Pt. In the same time, Tateishi et al. [187, 188] studied the electrochemical properties of ultrafine Pd particles (diameter, 2–10 nm) evaporated in vacuum on glassy carbon. They were able to distinguish between absorbed hydrogen and weakly and strongly adsorbed hydrogen. Attard and Banister [189], and Attard et al. [190] examined the electrochemical behavior of sub-monolayers and monolayers of Pd on Pt single crystals. Szpak et al. [191] used Pd electrodeposited on Au in their study on the role of interphase in charging of the Pd–H system. Cheek and O'Grady [142, 143], Gräsjo and Seo [144], as well as Yamamoto et al. [151] studied hydrogen absorption in thin Pd layers by the electrochemical quartz crystal microbalance.

However, it was Czerwiński and co-workers who consequently developed the idea of thin Pd layers for electrochemical studies on Pd. In 1991, they published the first papers devoted to the electrochemical behavior of Pd deposited on Au and reticulated vitreous carbon (RVC) [126, 127]. For the next 20 years, Czerwiński's group have published a series of systematic reports demonstrating the unique features of this approach for the examination of hydrogen electrosorption in Pd [53–56, 126–128, 143, 153, 190–200, 203, 204, 208] and many of its alloys [17–20, 54–56, 64–67, 146, 152–157, 201, 205–207, 209–240]. This idea has soon been adopted by other research groups, and since that time, numerous papers have appeared devoted to the studies on the electrochemical aspects of hydrogen insertion into thin Pd layers.

Baldauf and Kolb [241] studied the electrochemistry of ultrathin (1–100 atomic layers) Pd electrodeposits on Au single crystals. Wen and Hu [242–244] prepared PdO and Pd coatings on Ti electrodes by thermal decomposition and investigated hydrogen electrosorption from various solutions. Podlovchenko et al. [245] examined Pt-supported Pd electrodeposits of various degrees of dispersion (particle size, 25–1,200 nm). Manolatos and Jerome [246] prepared electrochemically Pd coatings on iron for hydrogen permeation studies. Li and Cheng [247] examined hydrogen solubility and diffusion in thin (0.022–0.135 μm) Pd layers fabricated by physical vapor deposition on Au-coated Ni matrix. Giacomini et al. [248] studied hydrogen oxidation and oxygen reduction reactions on Pd particles electrodeposited on polythiophene layers on glassy carbon. Winkler et al. [249] performed electrochemical studies on Pd–fullerene films formed from fullerene and Pd(II) acetate trimer. Safonova et al. [250], Rusanova et al. [204, 251], Roginskaya et al. [252], Plyasova et al. [253], Tsirlina et al. [254–256], and Petrii et al. [257] examined the properties of Pd electrodeposited on Pt or Au at various potentials and according to various deposition procedures. Bartlett et al. [258, 259] fabricated nanostructured Pd films (200 nm) by electrodeposition from lyotropic liquid crystalline phases on Au matrix and investigated various aspects of hydrogen electrosorption. Rose et al. [260] investigated hydride phase formation in carbon-supported Pd nanoparticles (average size, 14 nm) using electrochemistry, extended X-ray absorption fine structure (EXAFS), and X-ray diffraction (XRD). Paillier and Roué [261] characterized the structure (with XRD, X-ray photoelectron spectroscopy (XPS), and Rutherford backscattering spectroscopy) and the hydrogen electrosorption properties of nanostructured Pd thin films (7–27 nm) prepared by pulsed laser deposition. Liu et al. [148–150] used Pd and Pd–Ag films (120 nm) sputtered on a quartz crystal to study the kinetics of hydrogen or deuterium absorption in a Pd. Gabrielli et al. [174, 262–265], Łosiewicz et al. [266], Lasia [267], Birry and Lasia [268], Martin and Lasia [269, 270], as well as Duncan and Lasia [271–273] published numerous papers on hydrogen electrosorption in thin Pd deposits (starting from several monolayers to a thickness of 400 nm) devoted to the absorption mechanism and kinetics, influence of solution composition, and electrode substrate as well as the effect of surface poisons on hydrogen absorption. Denuault et al. [274] examined the electrochemical behavior of nanostructured Pd layers (thickness, 0.2–2 μm) electrodeposited from a liquid crystal phase on Pt. Frydrychewicz et al. [275–277] studied the electrochemistry of reticulated vitreous carbon–polyaniline–Pd composite electrodes prepared electrochemically as well as Pd nanodeposits on glass obtained in a dual-electrode sandwich system with a porous polycarbonate membrane. Chu et al. [278] described the procedures of the preparation of Pd nanoparticles and nanofilms (50–300 nm) by electroless deposition on ceramics. Bouhtiyya and Roué [279] presented structural, morphological, and electrochemical characterizations of Pd thin films (thickness, 10–300 nm; crystallite size, 7–15 nm) prepared by pulsed laser deposition. Lebouin et al. [280] examined hydrogen insertion into ultrathin (1–60 atomic layers) Pd films electrodeposited on Pt single crystals. Oliveira [281, 282] loaded with hydrogen Pd black films (1 or 8–9 μm) obtained via spontaneous deposition by dipping a Ni electrode in a Pd salt solution. Corduneanu et al. [283] electrodeposited nanoparticles, nanowires, and nanofilms on carbon and characterized them electrochemically and microscopically. Bertoncello et al. [284] prepared Pd nanoparticles embedded in a Nafion ultrathin film (15–75 nm) and studied their activity toward the electrooxidation of hydrogen. Scholl et al. [285] examined the surface morphology and electrochemical properties of Pd layers deposited on highly oriented pyrolytic graphite (HOPG) and Au. Skowroński et al. [286, 287] studied hydrogen electrosorption in sandwich Ni foam/Pd/carbon nanofiber electrodes. Stafford and Bertocci [138] applied the electrochemical quartz crystal microbalance to measure the stresses induced by hydrogen electrosorption into very thin (several monolayers) Pd deposits. Zhang et al. [288] presented the results of theoretical calculations of cyclic voltammetric profiles for hydrogen absorption and desorption in thin Pd layers and demonstrated a good agreement between their model and experimental data [126, 127]. Skitał et al. [289] described the mathematical model of the voltammetry in the potential region of hydrogen evolution/dissolution on/in a thin Pd electrode.

In Czerwiński's articles [198, 199, 202, 203, 208], the new type of Pd electrodes was originally named "limited volume electrodes" in order to emphasize their much smaller volume as compared with bulk Pd electrodes. Due to a limited diffusion field, the electrochemical response of LVEs is much more similar to that known for thin-layer electrodes [290, 291] rather than for systems under the conditions of semi-infinite diffusion. However, in contrast to a thin layer of electrolyte present in a typical thin-layer electrode, in the case of LVEs, the process of diffusion of electroactive species (hydrogen) occurs inside a solid. The volume of hydrogen-absorbing material can easily be controlled during the preparation of LVEs, which enables to study the absorption of a limited amount of hydrogen in electrodes of a limited and precisely known thickness. LVEs can be fast and fully loaded/deloaded with hydrogen, and the real absorption capacity of the material studied can be determined electrochemically in a simple way by the integration of hydrogen sorption or desorption currents. Under certain conditions, various forms of electrosorbed hydrogen can be distinguished. Moreover, surface processes

can be studied simultaneously with the bulk process of hydrogen dissolution, and the influence of the presence of various adsorbates on hydrogen insertion/removal can be examined. Vice versa, the effect of hydrogen insertion and removal on the surface electrochemical properties of Pd and its alloys can be studied.

Preparation and characterization of LVEs

Among various methods of metallic electrode preparation, such as metallurgic methods, vacuum deposition, chemical reduction, electroless deposition, and underpotential deposition, one of the most convenient and flexible methods of the preparation of Pd-based LVEs is electrochemical deposition. Pd can be deposited on a conductive, hydrogen-neutral matrix like gold or carbon, from aqueous solutions containing Pd salts, e.g., $PdCl_2$ with the addition of HCl or ammonia [53, 126–128, 143, 192–200, 202, 203, 208]. Deposition can be performed under galvanostatic or potentiostatic conditions using current densities of 1–2 mA cm^{-2} or potentials usually from the range 0.25–0.40 V vs. SHE. Since for the above deposition conditions the deposition efficiency of Pd is very close to 100% (above 97%, as determined using Faraday's law of electrolysis coupled with a classical gravimetry [126–128] or the electrochemical quartz crystal microbalance [55, 229]), the amount of deposited metal and its mean thickness can be controlled directly by the deposition charge. Typical values of deposit thickness used in LVE methodology are in the range 0.01–10 μm, which corresponds to approx. 50–50,000 atomic layers.

Electrochemical deposition has also been used effectively for the preparation of Pd alloy LVEs. Numerous papers have been published on the electrochemical behavior of Pd–Pt [54–56, 64, 66, 67, 153, 157, 205, 206, 212, 215, 218, 220–224, 228–231, 235, 238, 240]; Pd–Ni [146, 152, 201]; Pd–Au [55, 156, 207, 209, 228–231, 233, 235, 237, 238, 240]; Pd–Rh [17–20, 54–56, 64–67, 153, 154, 157, 214, 215, 218–224, 228–231, 237, 239, 240]; Pd–Ag [226, 232, 237]; Pd–Cu [232, 237]; Pd–Pt–Rh [54, 56, 64, 66, 67, 72, 153, 157, 210–213, 215–217, 220–222, 228–231, 236–238]; and Pd–Pt–Au [155, 225, 227, 230, 231, 237, 238] alloy electrodeposits, all in the form of LVEs. These alloys were deposited from baths obtained as a mixture of aqueous solutions of respective metal compounds, i.e., H_2PtCl_6, $HAuCl_4$, $RhCl_3$, $AgNO_3$, $CuNO_3$, $NiSO_4$. Both acidic (with HCl) and basic (with NH_3) baths were applied. By changing the bath composition and deposition conditions, alloys of various bulk compositions could be obtained. Using several deposition baths and applying a series of deposition potentials, it was possible to prepare Pd alloy LVEs in a wide composition range, covering the whole composition spectrum of the alloys able to absorb hydrogen.

Besides electrochemical techniques, like cyclic voltammetry, chronoamperometry, chronopotentiometry, electrochemical impedance spectroscopy, or electrochemical quartz crystal microbalance, used in the absorption experiment proper, electrodeposited LVEs have been characterized by a series of non-electrochemical methods. Fresh deposits as well as samples subjected to the electrochemical treatment, including hydrogen absorption, were examined by scanning electron microscopy, scanning tunneling microscopy, and Auger electron spectroscopy. These methods provided information on the surface state of the samples.

SEM and scanning tunneling microscopy (STM) images of freshly obtained electrodes revealed that properly prepared Pd-based deposits tightly covered the substrate, with no cracks present on the surface and the structure of the metal or alloy usually compact and grainy [18–20, 65, 155, 209, 217, 226, 227, 229, 232]. For the samples after hydrogen absorption procedure, some cracks appeared on the surface as a result of repeated hydrogen insertions and removal into/from the deposit. However, for pure Pd and most of its alloys with other noble metals (Pd–Au, Pd–Pt, Pd–Rh, Pd–Pt–Au, Pd–Pt–Rh, Pd–Ag), hydrogen penetration into the electrode bulk did not cause any considerable destruction of the deposit even after several hundreds of absorption/desorption runs [18–20, 65, 155, 209, 217, 226, 227, 229]. On the other hand, in the case of Pd–Cu alloys [232], hydrogen absorption led to a significant degradation of the alloy layer, probably due to high stresses accompanying hydrogen ingress into the alloy whose lattice parameter had been markedly reduced upon Pd alloying with Cu.

Using Auger electron spectroscopy (AES) technique, it was possible to examine the surface composition of Pd alloy LVEs [226, 227, 229, 232, 238]. It was demonstrated that Pd alloys with Pt, Au, and Rh are homogeneous on the surface on the scale of approx. 20 nm, i.e., AES point analysis with that lateral resolution did not detect any significant changes in alloy surface compositions between various places on the surface. This conclusion was in line with the electrochemical data, according to which a single voltammetric peak due to surface oxide reduction indicated alloy surface homogeneity. By a comparison between the electrochemical and surface spectroscopic data, an idea of the determination of surface composition of Pd ternary alloys was proposed [72, 229, 236, 238], which adapted the method established earlier by Rand and Woods for binary alloys [45, 292] based on a linear dependence of the potential of surface oxide reduction peak on alloy surface composition. On the other hand, in the case of electrodeposited Pd–Ag alloys, two surface phases were detected by cyclic voltammetry, mirrored by the presence of two

separate peaks due to surface oxide reduction on Pd-rich and Ag-rich phases [226, 232].

For the examination of the bulk properties of LVEs, methods such as energy-dispersive analysis of X-rays (EDAX), XRD, and atomic absorption spectroscopy (AAS) were applied [17–20, 54–56, 64–67, 72, 146, 152–157, 201, 205–207, 209–240]. Since in the case of noble metals the information depth in the EDAX technique (for a typical electron beam energy of 15 keV) is of the order of a micrometer, this method provides data on the bulk composition of Pd alloy LVEs. A major advantage of EDAX is the fact that this method is not destructive, so the analysis can be repeated many times, e.g., in order to follow changes in the composition of a given sample during the experimental procedure, and enables the examination of various zones over the sample. However, in some cases (e.g., Pd–Rh alloys), strong overlapping of peaks of the component elements in the X-ray spectrum makes it difficult to obtain reliable data on alloy composition. Moreover, for very thin layers, the results of the EDAX analysis may be affected by signals originating from the material used as a matrix for the deposit. Therefore, in such cases, for a precise determination of alloy bulk composition, the LVE deposits were dissolved in aqua regia and the solutions obtained were analyzed by the AAS technique. This method enables determining not only alloy bulk composition within the entire sample but also the exact amounts of particular alloy components. The latter fact is very important when the deposition efficiency is unknown and Faraday's law cannot be used. However, a major disadvantage of the AAS method is the fact that it is destructive and therefore the analysis can be performed only once for a given sample. It also provides average alloy composition and is insensitive to local changes in alloy composition resulting from surface or bulk segregation.

In order to obtain structural information on alloy electrodeposits, the XRD technique was employed [216, 226]. In the case of Pd–Pt–Rh alloys, the XRD signals were shifted into higher angles, as compared with the position typical of pure Pd without additional peaks in the position typical of other components. Therefore, it was concluded that a homogeneous solid solution was obtained characterized by a contracted crystal lattice, as compared with pure Pd [216]. On the other hand, XRD measurements performed on electrodeposited Pd–Ag alloys [226] revealed the presence of two series of signals placed between the peaks for pure Pd and Ag, which indicated the existence of two separate phases in the electrode bulk, i.e., an Ag-rich one and a Pd-rich one.

The bulk homogeneity of Pd alloys with Pt, Rh, and Au prepared as LVEs was confirmed by hydrogen absorption experiments [18, 19, 154–156, 201, 205–207, 216, 222, 224, 227, 231, 233–235, 237–239]. In the course of the relationship between the amount of absorbed hydrogen (hydrogen-to-metal atomic ratio, H/M) and electrode potential, a single region of the α–β phase transition was observed. The potential of the phase transition correlated with alloy bulk composition obtained by the EDAX or AAS methods, which indicated that the hydrogen-absorbing phase was the only phase present in the alloy [222, 231, 233, 234, 238]. It was proposed that this correlation could be utilized for the determination of alloy bulk composition of a Pd-rich alloy directly in the electrochemical experiment. This method enables an in situ, non-destructive analysis even for very thin layers, i.e., when other methods cannot be applied. A careful inspection of the shape of H/M vs. potential curve in the region of the phase transition allows checking whether bulk phase segregation has occurred in the system studied. In such a case, more phase transition regions appear on the H/M vs. potential curve (when new phases can absorb hydrogen), and/or the initial phase transition potential is shifted (when the additional phase does not absorb hydrogen) [216].

Another technique used at the stage of preparation and preliminary characterization of LVEs is the electrochemical quartz crystal microbalance (EQCM). By recording the response of the EQCM during metal or alloy deposition, one can easily monitor the deposition process in real time [55, 229]. The mass of deposited metals can be calculated via the Sauerbrey equation, and the deposition efficiency can be determined if the deposition charge and alloy composition are known.

Electrochemical studies on hydrogen sorption in Pd LVEs

Electrochemical procedures for the examination of hydrogen sorption in LVEs

A hydrogen absorption experiment can be realized under two different types of conditions, i.e., with permeable or impermeable boundaries, also called transmissive and reflective conditions, respectively [293–296]. In the former experimental setup, hydrogen enters the electrode on one side, diffuses through the metal, and desorbs on the other side, while in the latter one, hydrogen cannot be transferred across the electrode and may enter and leave the metal through the same phase boundary. In the case of Pd LVEs prepared as electrodeposits on a hydrogen-inert substrate, the studies are performed under the reflective (impermeable) conditions.

In an electrochemical experiment with the use of a LVE, the metal or alloy can be totally saturated with hydrogen in a short period of a cathodic polarization either at constant potential/current or during a cathodic voltammetric scan, while absorbed hydrogen can be extracted in a reverse oxidation process. From the charges obtained during

sorption/desorption, the amount of electrosorbed hydrogen can be calculated.

In numerous studies [202, 203, 207, 208, 212, 220], chronoamperometric absorption of hydrogen was coupled with voltammetric oxidative desorption. Hydrogen was introduced into Pd LVEs at various potentials and oxidized at various scan rates. As a result, the dependence of the electrochemically measured amount of sorbed hydrogen as a function of potential and scan rate could be examined.

In other experiments [155, 216], a procedure was applied which consisted of two series of chronoamperometric jumps between the potential into the region where neither absorbed nor adsorbed hydrogen exists and the potential located in the hydrogen absorption region. Thus, it was possible to determine the amount of hydrogen absorbed as a function of potential during the absorption run together with the amount of hydrogen still remaining in the alloy at various potentials during the desorption run. As a result, H/M vs. the potential plots obtained were analogous to the concentration vs. pressure curves known for the experiments with increasing or decreasing hydrogen pressure under the gas phase conditions. This procedure enabled to study electrochemically the phenomenon of hysteresis [19, 154, 155, 216, 224, 226, 231, 233–235, 237–239]. Additionally, from the analysis of the current–time responses recorded during hydrogen extraction, the time necessary for a complete hydrogen insertion or removal as well as hydrogen diffusion coefficient in the electrode material could be determined [19, 146, 154, 155, 206, 216, 231, 235, 237, 239]. Moreover, by identifying the characteristic inflection points on the chronoamperometric curves corresponding to the phase transitions, it was possible to determine the limiting amounts of hydrogen in the α- and β-phases [235, 239].

In order to avoid the effects of electrode aging during hydrogen insertion/removal in the experiment proper [155, 233, 234, 297], freshly deposited Pd-based LVEs were usually subjected to a series of chronoamperometric and voltammetric runs in the hydrogen region until a steady-state voltammogram was obtained.

Influence of electrode potential on the amount of absorbed hydrogen

A typical dependence of the amount of hydrogen electrosorbed in Pd on electrode potential consists of three characteristic regions, determined by the presence of particular forms of sorbed hydrogen (Fig. 3). First, the amount of sorbed hydrogen rises slowly with decreasing potential, which corresponds to hydrogen adsorption and the α-phase formation. Then, a sharp increase in the H/Pd ratio is observed in a narrow potential range due to the α–β phase transition. At room temperature, the

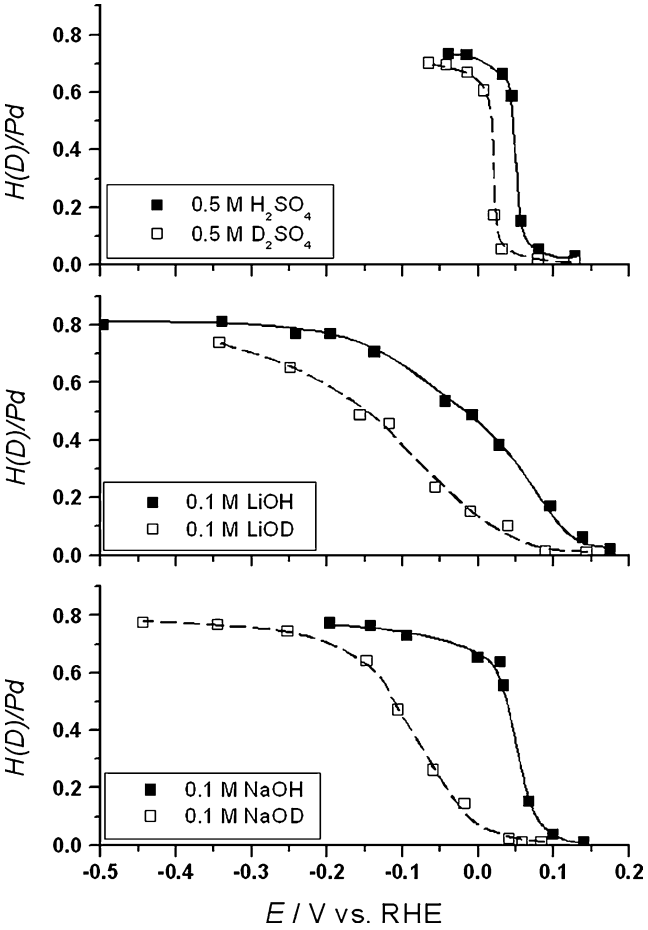

Fig. 3 Influence of electrode potential on the amount of absorbed hydrogen and deuterium in Pd LVE (thickness, 0.8 μm) in acidic [85] and basic solutions [127] at room temperature. Scan rate during absorbed hydrogen electrooxidation, 0.01 Vs^{-1}

potential of the α–β phase transition is equal to 50 mV [3, 298, 299] vs. the RHE in the working solution. In alkaline solutions, the width of the phase transition region is greater and the slope of the H/Pd vs. potential curve depends on the kind of cation present in the solution [127, 128, 194, 196, 197, 199, 200] (see the next section). At lower potentials, the absorption capacity again slowly increases due to the absorption in the β-phase with a small contribution from hydrogen adsorption.

The general shape of H/Pd vs. potential curve is similar to the pressure–concentration curve known for hydrogen absorption from the gas phase [3]. In the region of hydrogen absorption in the α-phase, the electrode potential is proportional to the logarithm of the H/Pd atomic ratio. This relationship is equivalent to Sieverts' equation known for the absorption from the gas phase [300].

As demonstrated by Lewis and Flanagan [116–118] as well as Vasile and Enke [298] for potentials higher than the hydrogen evolution potential, the electrode potential

under the electrochemical conditions corresponds to hydrogen pressure in the gas phase experiments. According to the Nernst equation, a decreasing potential is equivalent to an increasing hydrogen gas pressure. The scheme of electrochemical cell and the electrode reactions proceeding during the hydrogen electrosorption experiment in Pd can be described as follows:

$$\mathrm{Pt,H_2|H^+|H}_x\mathrm{Pd}_y$$

$$\text{Pd working electrode}: x\mathrm{H}:y\mathrm{Pd}+\mathrm{H}^+ + \mathrm{e}^- \rightarrow (x+1)\mathrm{H}:y\mathrm{Pd} \quad (1)$$

$$\text{Pt reference electrode}: \frac{1}{2}\mathrm{H_2} \rightarrow \mathrm{H}^+ + \mathrm{e}^- \quad (2)$$

$$\text{Overall reaction}: x\mathrm{H}:y\mathrm{Pd}+1/2\mathrm{H_2} \rightarrow (x+1)\mathrm{H}:y\mathrm{Pd} \quad (3)$$

The measured potential of the cell is given by the expression:

$$E = E_{\mathrm{PdH}} - E^0_{\mathrm{H2/H+}} - [(RT)/(2F)]\ln\left[(a_{\mathrm{H+}})^2/p_{\mathrm{H2}}\right] = E_{\mathrm{PdH}}(\text{vs. RHE}) \quad (4)$$

The potential of a Pd electrode referred to the RHE can be converted into hydrogen pressure [116–118, 298, 299].

$$p = \mathrm{e}^{-2\cdot F\cdot E/R\cdot T} \quad (5)$$

In particular, the potential of the α–β phase transition on the RHE scale corresponds to the equilibrium plateau hydrogen pressure connected with the reaction equilibrium constant of the hydride formation.

As discussed by Dębowska and Baranowski [301], the potential of a hydrogen-saturated Pd electrode can be directly related to the corresponding pressure of gaseous hydrogen only for values not exceeding the external pressure. On the other hand, when the electrode potential is below the hydrogen evolution potential, the above thermodynamic relation between potential and hydrogen pressure cannot be applied. The relations between electrode potential and the equivalent hydrogen pressure were discussed in detail in the literature [267, 268, 302–307]. As noted by Zoltowski [300], only homogeneous (i.e., where a single phase of absorbed hydrogen is present) and stress-free hydrogen–metal systems may be (but in some cases they are not) in a true (thermodynamic) equilibrium.

Birry and Lasia [268] as well as Vigier et al. [308] noted that hydrogen generated in the solution even at potentials positive to the hydrogen evolution potential could affect the determination of hydrogen absorption isotherm in an electrochemical experiment. To avoid the problem of the accumulation and subsequent oxidation of hydrogen from the solution, they recommended the application of a hydrodynamic flow forced around the electrode by electrode rotation or solution stirring. On the other hand, Czerwiński et al. [202, 203] and Grdeń et al. [206] concluded that the amount of hydrogen absorbed in the Pd electrode was not influenced by the evolution of hydrogen gas formed simultaneously with hydrogen absorption. Lawson et al. [309] did not find any difference between the charge needed for the oxidation of absorbed hydrogen in Pd when the experiments were performed in hydrogen and in a neutral (Ar) atmosphere.

The plots of the H/Pd ratio vs. potential obtained from stationary absorption/desorption experiments coincide in the regions of the α- and β-phases, but differ in the phase transition region, with the β→α transition placed at a slightly higher potential than the α→β transition. This behavior corresponds to the effect of hysteresis known for gas phase measurements where the hydrogen pressure connected with the α–β equilibrium during desorption course is lower than during absorption [1, 3, 310–316].

Influence of electrolyte composition

In [126–128, 192–194, 196–200, 202, 203, 208], hydrogen electrosorption in Pd LVEs from acidic and basic solutions was compared. The main differences between both kinds of electrolytes are as follows (see also Figs. 2, 3, 4, 5):

1. The source of hydrogen is different in acids (H^+ ions) and in bases (H_2O molecules).
2. The potential range of hydrogen electrosorption in bases is shifted negatively on the SHE scale as compared with acids.
3. The rate of hydrogen uptake from bases is slower than in the case of acids.
4. The processes of hydrogen absorption/desorption in bases are electrochemically much more irreversible than in acids.
5. The process of the α–β phase transition in bases occurs in a wider potential range than in acids.
6. The maximum amount of absorbed hydrogen in bases is slightly greater than in acids.
7. The process of hydrogen electrosorption in bases depends strongly on the kind of alkali metal cations present in the solution.
8. The process of hydrogen electrosorption in bases depends on the electrode history.

It was demonstrated [194, 197, 200] that in contrast to acidic solutions, in LiOH and NaOH solutions, the α-phase is more readily oxidizable (i.e., its oxidation starts at lower potential) than the β-phase. This behavior indicates a strong electrochemical irreversibility of the processes of hydrogen absorption in the β-phase and its desorption in some basic media. However, in KOH and CsOH solutions, the order of

the oxidation of a particular phase of absorbed hydrogen is inverted, with the β-phase easier to be oxidized than the α-phase [194, 197]. Therefore, it was concluded that the interactions between Cs and absorbed hydrogen in the α- and β-phases in Pd are totally different from Li–H interactions [200]. This fact is a manifestation of the general influence of the kind of alkali metal cation present in basic solution in the process of hydrogen electrosorption.

The process of hydrogen uptake in bases is slower than in acids and proceeds according to a different mechanism of hydrogen atom generation. In the former case, hydrogen originates from the reduction of H^+ ions, while in the latter case it is generated from and then oxidized back to water molecules [203].

The shape of the H/Pd vs. potential relationship for basic solutions strongly depends on solution composition and differs significantly from the shape of analogous plots obtained in acidic solutions [194, 197, 199, 200]. The region corresponding to the phase transition is much wider and the slope of the H/Pd vs. potential plot during the phase transition is lower, i.e., the curve is not as vertical as in acidic solutions (Fig. 3). The width of the phase transition region in basic solutions ranges from approx. 50 to 200 mV as compared with only several millivolts in acidic solutions. The slope of the phase transition region changes with the kind of alkali metal cation present in the solutions, increasing in the order: LiOH < NaOH < KOH < CsOH [197]. The maximum H/Pd ratios in basic solutions are by 5–10% higher than in acids and also depend on the solution composition, decreasing with increasing size of the alkaline metal cation present in the solution [197, 199]. All the effects are not observed in acidic solutions upon the addition of alkali metal cations (Figs. 4 and 5).

According to Gibbs' phase rule, a not vertical region of the α–β phase transition observed in basic solutions suggests that in the presence of alkali metals, the Pd–H systems have an additional degree of freedom, which is absent in acidic solutions. This effect may be due to the increase in the number of components resulting from the incorporation of alkali metals into Pd bulk during hydrogen absorption from basic solutions, which requires potentials low enough for the alkali metal deposition to occur. The incorporation of alkali metals into Pd was confirmed by the examination of the composition of Pd LVEs by atomic absorption spectroscopy [203] and neutron activation analysis [196, 200].

Another effect limited to the basic solution concerns the influence of the electrode history on the course of H/Pd vs. potential plots [194, 199, 200]. The amounts of absorbed hydrogen obtained during a successive decrease in absorption potential were compared with those obtained with increasing potential from the negative side. In acidic solutions, the experimental points obtained in both procedures lay on the same line, and no changes in the amount of absorbed hydrogen or the position of the phase transition region were observed. On the other hand, in the case of hydrogen absorption form basic solutions, both H/Pd vs. potential plots did not coincide and their course depended on whether the absorption was performed in the direction of increasing or decreasing potentials. The direction of the change in the potential of the phase transition was different for different cations [194, 199, 200].

It was concluded [127, 193–200, 203] that in the presence of alkali metal cations in a basic solution, hydrogen insertion and removal into/from Pd accompanied by alkali metal incorporation causes irreversible changes in the Pd lattice, which have further influence on hydrogen absorption/

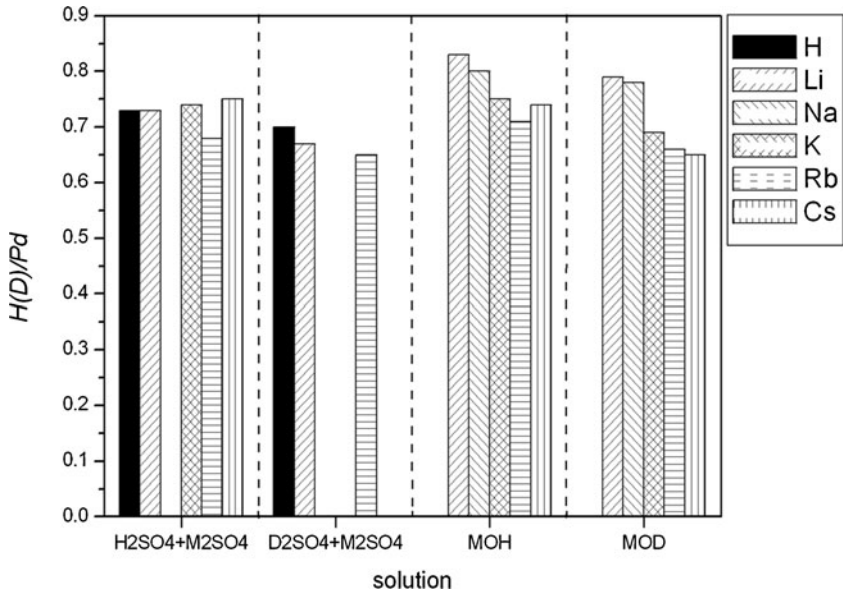

Fig. 4 Influence of solution composition on the maximum amount of hydrogen and deuterium absorbed in Pd LVEs (thickness, 0.8 μm) at room temperature [199]

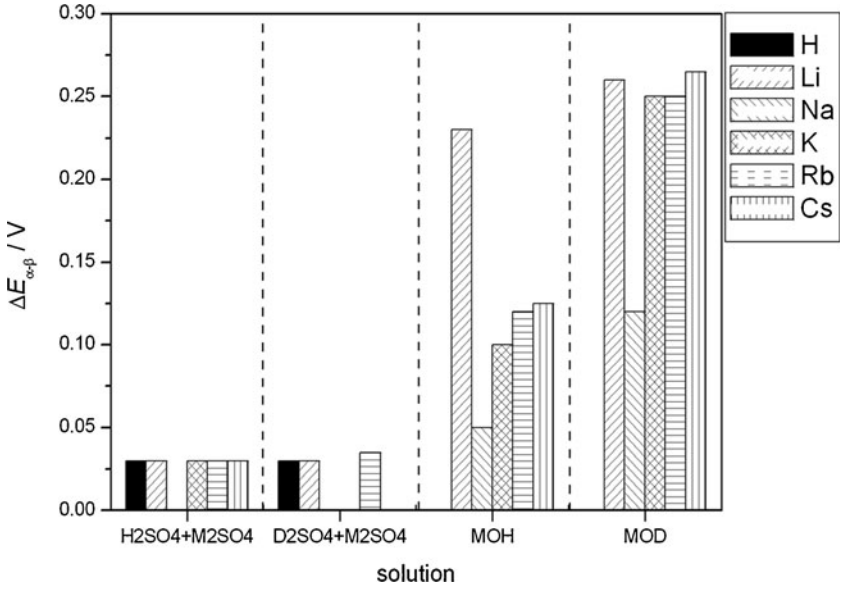

Fig. 5 Influence of solution composition on the width of the α–β phase transition region for hydrogen and deuterium absorption in Pd LVEs (thickness, 0.8 μm) at room temperature [199]

desorption processes. It should be stressed that the aforementioned effect of the electrode history on the course of H/Pd vs. potential plot cannot be identified with the hysteresis effect described in "Influence of electrode potential on the amount of absorbed hydrogen." The latter phenomenon has a different origin and occurs also in acidic solutions.

Isotopic effect

In [126–128, 192–200, 202, 203], hydrogen and deuterium electrosorption into Pd LVEs from acidic and basic solutions were compared. Under conditions of a cyclic voltammetric experiment in acidic media, it was observed that the potential region of deuterium sorption was shifted into lower potentials as compared with the hydrogen sorption. The isotopic effect was larger for the α-phase than for the β-phase formation. The weaker isotopic effect in the latter case was attributed to the fact that the diffusion coefficient of deuterium in bulk Pd is about 30% higher than that of hydrogen, while in the α-phase it is much lower than in the β-phase [219].

The negative shift of the α–β phase transition potential means that the formation of Pd deuteride requires more energy than the hydride formation and, therefore, the β-phase of deuterium in Pd is thermodynamically less stable. The data obtained for Pd LVEs are consistent with the results for bulk Pd reported by Flanagan [118], according to whom the α–β phase transition occurred at 31 mV vs. RHE in heavy water acidic solution and at 50 mV in light water. However, the slopes of the H/Pd vs. potential curves in the phase transition regions were identical for deuterium and hydrogen. The maximum amount of absorbed deuterium was lower than that of Pd, but did not depend on acidic solution composition, either [128, 199].

In basic solution, the overall trends due to the isotopic effect were qualitatively similar to acidic solutions, however with the additional effect of solution composition [128, 194, 196, 197, 199, 200]. For each kind of alkali metal cation present in the solution, the phase transition region for deuterium absorption was shifted negatively with respect to that for hydrogen, but this shift was four to five times higher than in acidic solutions. Moreover, the slope of the D/Pd vs. potential dependence usually changed as compared with the H/Pd vs. potential plot. For instance, the width of the phase transition region for deuterium absorption increased in the order: NaOD < KOD < LiOD < CsOD, while for hydrogen, it was as follows: NaOH < KOH < CsOH < LiOH [197, 199]. The maximum value of the D/Pd ratio was lower than the H/Pd ratio for the same cation and strongly depended on the solution composition, decreasing with increasing size of alkali metal cation. An isotopic effect was also observed in the case of the rate of hydrogen absorption, where the time needed for Pd saturation with deuterium was more affected by the solution composition than in the case of the saturation with hydrogen. The relative rates of deuterium absorption were in the order: NaOD > CsOD > LiOD > KOD, while for hydrogen absorption, the relation was different: LiOH = CsOH = NaOH > KOH [197]. Similar to hydrogen absorption, also in the case of deuterium, an influence of electrode history on the course of the D/Pd vs. potential plot was observed in basic solutions in heavy water [197, 199, 200].

Influence of electrode thickness

The studies on the effect of a Pd film thickness on their absorption behavior started with the report by Horkans [181] who concluded that thinner Pd layers (thickness in

the range 50–1,000 nm) could absorb more hydrogen than bulk Pd samples; however, they lose this ability on annealing. Frazier and Glosser [179] found a strong dependence between Pd layer thickness (6–120 nm) on the amount of absorbed hydrogen, but with the limiting β-phase concentration decreasing with decreasing film thickness. On the other hand, Rosamilia et al. [186] did not observe any difference in the amount of hydrogen absorbed in layers of a thickness in the range 1–10 μm. Baldauf and Kolb [241], studying hydrogen electrosorption in ultrathin Pd deposits, found that Pd ability to absorb hydrogen started from three atomic layers and the amount of absorbed hydrogen increased with increasing film thickness, reaching a limiting value of H/Pd = 0.6 above 100 atomic layers. Tateishi et al. [187, 188] found that the amount of absorbed hydrogen in ultrafine (2- to 10-nm diameter) Pd particles supported on glassy carbon decreased with a decrease in the particle size, from H/Pd approx. 0.6 for large particles to below 0.2 for small particles. Podlovchenko et al. [245] found that the amount of hydrogen absorbed in dispersed Pd deposits (particle size, 25–1,200 nm) was higher than that of smooth Pd and differed for various dispersed forms of Pd due to the variation of the number of defects inside the metal.

With the use of LVEs, Czerwiński et al. [126–128, 202, 203, 208] began systematic studies on the influence of electrode thickness on the amount of absorbed hydrogen in Pd. Their first reports [126–128] concerning Pd layers thicker than 0.8 μm suggested that the thickness of Pd LVEs had no effect on their absorption capacity. However, further, studies on that effect for smaller electrode thickness together with the examination of the effect of scan rate on the amount of electrochemically oxidized hydrogen revealed a significant influence of electrode thickness on the absorption behavior of Pd LVEs [202, 203, 208].

Hydrogen and deuterium absorption in Pd LVEs in the thickness range from 0.2 to 3.2 μm was investigated in acidic and basic solutions [202, 203, 208]. A characteristic shape of the dependence of the electrochemically measured amount of absorbed hydrogen on scan rate was observed with a maximum of H(D)/Pd ratios at scan rates usually between 0.01 and 0.02 V s^{-1} A significant effect of the electrode thickness on the shape of H(D)/Pd vs. scan rate dependence was found. With the decrease in the thickness from 3.2 to 0.2 μm, the maximum H/Pd or D/Pd ratios increased from 0.74 to 0.87 and from 0.70 to 0.85, respectively, in acidic solutions, and from 0.65 to 0.88 and from 0.66 to 0.86, respectively, in basic solutions. The position of the maximum on H(D)/Pd ratio vs. the scan rate plot shifted toward lower scan rates with the increase in the electrode thickness becoming much less pronounced for thicker electrodes. The depletion with hydrogen at very slow scan rates was more significant for thinner electrodes in acidic solutions, while for basic solutions an opposite effect was observed. The lowest amount of hydrogen and deuterium for the thinnest layers in acidic solutions corresponded to H(D)/Pd ratios of 0.68 and 0.62, respectively, and for the thicker layers in basic solutions corresponded to H(D)/Pd ratios of 0.55 and 0.65, respectively. The decrease in the electrochemically measured amount of hydrogen or deuterium observed at fast scan rates was generally greater for thicker electrodes. Moreover, in basic solutions, the maximum H(D)/Pd ratios decreased with increasing size of the alkali metal cation present in the electrolyte. In general, the dependence of the electrochemically measured amount of hydrogen or deuterium on the scan rate was similar for both isotopes, although the exact position of the H(D)/Pd maximum and the maximum H(D)/Pd values were not the same, suggesting some differences in the behavior of hydrogen and deuterium in thin Pd layers.

These experimental facts were explained by a model of hydrogen electrosorption in Pd LVE with a key role of a thin layer of hydrogen accumulated just below the electrode surface in a subsurface region, where the hydrogen concentration would exceed that in the bulk of Pd. At small electrode thickness, hydrogen absorbed in the subsurface layer contributes significantly to the total amount of hydrogen in the metal. According to Czerwiński's model of a dual mechanism of hydrogen desorption, involving electrochemical oxidation and non-electrochemical hydrogen recombination, the relative rates of both paths of absorbed hydrogen removal depend on the scan rate and electrode thickness; for each thickness, there is an optimal scan rate at which all absorbed hydrogen is removed via the electrochemical oxidation and can be measured in a cyclic voltammetric experiment [202, 203, 208].

The effect of electrode thickness on the amount of absorbed hydrogen was also studied by Gabrielli et al. [263]. They observed an increase in the H/Pd ratio with decreasing electrode thickness, from 0.61 for 1.75 μm to 0.71 for several monolayers. The lower values of H/Pd ratio as compared with the maximum results from [202] may be attributed to the use of lower scan rates, for which due to the importance of the non-electrochemical desorption path, not all absorbed hydrogen could be measured electrochemically. Paillier and Roué [261], who studied the hydrogen electrosorption properties of nanostructured Pd thin films (7–27 nm), also reported that for thinner Pd films, the hydrogen solubility was greater. H/Pd values changed from 0.32 for a thickness of 27 nm to 0.48 for 7 nm, without a significant effect from the scan rate. In contrast, Duncan and Lasia [272] did not find any effect of Pd layer thickness between ten monolayers and 60 nm on the amount of absorbed hydrogen in Pd.

On the other hand, many results on hydrogen absorption in Pd clusters or nanocrystalline Pd show that for small Pd particles, the ability to absorb hydrogen is markedly weaker than for bulk Pd and decreases with decreasing particle size. For instance, Lebouin et al. [280] studied the influence of electrode thickness on hydrogen solubility in Pd films (1–60 atomic layers) electrodeposited on Pt single crystals. They found that the maximum H/Pd ratio was significantly lower than for bulk Pd and decreased with decreasing film thickness, being equal to 0.45 for 16 monolayers and 0.3 for 10 monolayers of Pd. A similar tendency was observed by Züttel et al. [317] for nanometer Pd clusters. These results imply that there may be an optimal thickness of a Pd layer for which the hydrogen solubility attains a maximum. However, a detailed discussion on the unique absorption properties of small Pd clusters or ultrafine nanostructures is out of the scope of this paper, and we refer the reader to the literature [317–328].

Influence of temperature

Temperature is an important parameter affecting the process of hydrogen absorption in Pd. According to the phase diagram of the Pd–H system, with the increase in temperature, the miscibility gap gradually decreases and finally disappears at the critical temperature. Gas phase experiments show that the plateau pressure corresponding to the phase transition increases with temperature, while the maximum amount of hydrogen absorbed in the β-phase decreases. This behavior is in line with the fact that hydrogen absorption in Pd is an exothermic process, and therefore at higher temperatures, the reaction equilibrium shifts toward desorption. The hysteresis effect also tends to decrease with increasing temperature.

Czerwiński et al. [208] studied the influence of temperature (in the range 373–341 K) on hydrogen and deuterium sorption in Pd LVEs of various thicknesses (from 0.2 to 1.6 μm) from acidic and basic solutions. They observed a greater electrochemical reversibility of hydrogen absorption/desorption at elevated temperature. A similar effect was observed by Hubkowska et al. [233, 234] for Pd and Pd alloys with Au and Pt, as well as Koss et al. [239] for Pd-Rh alloys. Zhang et al. [329] also reported on the effect of temperature increase on the acceleration of the hydrogen sorption process in Pd under both galvanostatic and potentiostatic charging conditions.

The influence of scan rate on the electrochemically measured H/Pd ratio at various temperatures was also examined [208]. For all temperatures, a maximum H/Pd ratio at scan rates between 5 and 15 mV s^{-1} was observed. With increasing temperature, this maximum became less pronounced and was shifted to lower scan rates. The maximum H/Pd ratio decreased with temperature, more strongly for thinner electrodes and for acidic than for basic solutions.

The influence of temperature on the course of the H/Pd vs. scan rate dependence was interpreted as a consequence of a different temperature effect on the rate constants of two concurrent hydrogen desorption reactions. Temperature variation changes the relative importance of both hydrogen desorption paths. With increasing temperature, the electrochemical desorption becomes predominant and less hydrogen may escape without charge transfer, which leads to a weaker dependence of the hydrogen oxidation charge on scan rate. It is also possible that temperature may change the rate-determining step of hydrogen desorption and influence the energetics of various forms of hydrogen adsorbed on the electrode surface.

In the case of deuterium absorption the general influence of temperature was similar to that for hydrogen, however, with some quantitative differences between the effects for both isotopes. The maximum amount of deuterium absorbed in Pd LVE decreased with temperature more rapidly than the amount of absorbed hydrogen. For temperatures lower than 310 K, maximum hydrogen concentration was slightly greater than that of deuterium, while at higher temperatures, the opposite tendency was observed and the concentration of deuterium was greater. The latter effect was not present for gas phase experiments in bulk Pd, where in the same temperature range the H/Pd ratio was always higher than the D/Pd ratio. Therefore, it was concluded that the behavior of hydrogen and deuterium absorbed in Pd LVEs was different from that typical of Pd samples of a large volume. It that contex, possible differences between the thickness and concentration of hydrogen/deuterium in the subsurface layer were taken into account, playing a major role in the hydrogen absorption/desorption process in thin Pd layers [208]. A weaker temperature dependence of the deuterium absorption capacity can also be ascribed to the less exothermic process of deuterium absorption in comparison with that of hydrogen.

A different temperature effect on hydrogen absorption from acidic and basic solutions was explained by a different rate of alkali metal incorporation from basic solution at various temperatures. With increasing temperature, this process should occur faster, and the concentration of alkali metals beneath the surface of Pd as well as their penetration depth probably increase. This fact may affect in a greater extent the properties of subsurface hydrogen and enhance the stability and concentration of hydrogen in that phase, which leads to a weaker temperature dependence of hydrogen solubility in Pd LVEs in basic solutions as compared with acidic solutions [208].

Hubkowska et al. [233, 234] studied the influence of temperature on the position of the phase transition region on the potential scale. They found a decrease in the potentials of both the α→β and β→α phase transitions

with increasing temperature. From the temperature dependence of those potentials, the thermodynamic parameters of hydrogen absorption and desorption were determined. Similar to earlier findings, the increase in absorption/desorption rate with temperature was observed, mirrored in higher electrosorption current, shorter loading/deloading times, and lower potential of hydrogen oxidation peak.

Influence of preparation conditions on hydrogen sorption in Pd deposits

In most aforementioned studies performed with the use of Pd electrodeposits, the values of deposition current or potential during Pd LVE preparation were limited to conditions under which hydrogen sorption into the deposit being formed could be avoided. However, Pd deposits formed in the presence of absorbing hydrogen exhibit numerous interesting features, and their absorption behavior markedly differs from that of normal samples.

Safonova et al. [250], Rusanova et al. [204, 251], Roginskaya et al. [252], Plyasova et al. [253], Tsirlina et al. [254–256], and Petrii et al. [257] examined the influence of deposition conditions on the properties of thin (1–2 μm) Pd layers. They prepared a series of Pd electrodeposits from chloride solutions at three potential ranges: (1) at potentials where no kind of hydrogen sorption occurs, (2) in the region of hydrogen absorption in the α-phase, and (3) in the region of hydrogen absorption in the β-phase.

The ability of Pd layers to absorb hydrogen was strongly dependent on the deposition potential. The deposits obtained in the absence of any kind of simultaneous hydrogen sorption exhibited hydrogen absorption properties very close to those typical of polycrystalline Pd. On the other hand, the samples prepared with a parallel formation of the β-phase were characterized by very high absorption capacities, with an anomalously high hydrogen concentration in both the α- and β-phase. In the latter case, the maximum H/Pd ratio exceeded unity, reaching 1.2 for Pd deposited at 0.026 V vs. RHE [252, 257]. The length of the α–β transition plateau was higher than for normal Pd samples. Moreover, the potential of the α–β phase transition was also dependent on the deposition potential and decreased by approx. 3–10 mV for Pd samples formed in the β-phase potential region. However, a further decrease in the deposition potential toward hydrogen evolution potential resulted in a substantial deterioration of the absorption capacity of Pd deposits, with the maximum H/Pd ratio reaching only 0.4.

The increased hydrogen absorption ability for Pd deposited with a simultaneous hydrogen uptake was attributed to the anomalous structure of such deposits. The structural peculiarities of Pd deposits obtained under hydriding conditions were studied by STM, XRD, and XPS [251–254]. The anomalously high hydrogen concentrations and the difference in the course of hydrogen absorption isotherms were correlated with the highly defective structure, which was obtained due to Pd lattice deformation during its growth accompanied by hydrogenation. These deposits were characterized by higher real surface area, which resulted not from a smaller crystallite size but from a low degree of their coalescence. These features were ascribed to the mechanism of deposit formation with a simultaneous β-phase generation.

Similar tendencies were also reported for deuterium absorption in Pd deposits formed at various potentials [204]. However, due to the isotopic effect, the amount of deuterium absorbed at a given potential was lower than the corresponding concentration of hydrogen. Moreover, the dependence of the ratio between hydrogen and deuterium concentration on the absorption potential was different from that observed for normal Pd samples.

Increased hydrogen solubilities with H/Pd ratio close to unity were also observed for Pd prepared by means of quasitemplate electrodeposition from chloride solutions with the addition of some polymers, like polyethylene glycol and polyvinyl pyrrolidone [256]. The effect on the enhanced absorption capacity was visible for higher molecular weights of those polymers. According to Tsirlina et al. [256], the reasons for the unusual absorption properties of those materials were both the specific structure and the effect of polymer inclusions. They noted that the solvation of Pd metal nuclei by polymeric molecules could result in further deposit growth only in selected directions without the tendency to coalescence. Moreover, the presence of polymeric surfactants seems to also affect the bulk defectiveness of Pd deposits. Thus, the authors concluded that by combining the proper adjustment of the deposition potential with optimal additives of surfactants, it may be possible to prepare Pd deposits with unique hydrogen sorption properties.

H/Pd ratios approaching unity were also reported by Frydrychewicz et al. [275] for hydrogen absorption in Pd electrodeposited in a dual-electrode sandwich system containing two indium tin oxide-coated glass electrodes separated by a porous polycarbonate membrane filled with chloride solution. Such deposits were highly dispersed and exhibited increased hydrogen absorption capacity. The authors related these properties to the special conditions of deposit formation, under which the growing Pd deposit feels a considerable mechanical pressure provided by the compressed membrane.

Frydrychewicz et al. [276, 277] also studied hydrogen absorption behavior of multi-component electrodes composed of RVC, polyaniline, and Pd. In that case, the amount of hydrogen absorbed in the β-phase was distinctly smaller than in Pd deposits on bare RVC. This effect was attributed

to the specific features of Pd distribution in the composite material, where Pd crystals became electrically separated from RVC by isolating the layer of polyleokomeraldine in the course of hydrogen sorption.

An anomalously high absorption capacity with H/Pd ratio above 1 was also reported by Rose et al. [260] for carbon-supported Pd nanoparticles (average size, 14 nm) electrolytically loaded with hydrogen. However, XRD and EXAFS measurements did not confirm such high hydrogen uptake, and H/Pd ratios below 0.7 were obtained from the crystallographic data. High loading with hydrogen was reported by Oliveira [281] who was able to reach H/Pd ratio above 2 in Pd–black films (thickness, approx. 1 μm) spontaneously deposited on Ni. The hyperstoichiometric hydrogen was attributed to hydrogen gas trapped in surface voids, as the structural data suggested the normal β-phase formation with H/Pd ratio equal to 0.79.

Electrochemical studies on hydrogen sorption in Pd alloys prepared as LVEs

Before the application of LVE methodology, only few reports were devoted to the electrochemical behavior of Pd alloys in the potential region of hydrogen electrosorption [173, 182, 183, 186]. Usually, the polarization of Pd-based electrodes in the form of wires, foils, sheets, etc., into the potentials of hydrogen absorption was avoided due to the aforementioned complications connected with the generation of high-magnitude currents. However, the use of LVEs opened new possibilities for studying hydrogen electrosorption in Pd alloys. Since the end of the 1990s, numerous papers have been published [55, 64, 66, 67, 146, 152–157, 201, 207, 209–217, 220–228, 230–235, 237–240, 308, 330–338] on hydrogen electrosorption in Pd binary and ternary alloys with such metals as Pt, Ni, Au, Rh, Ag, Cu, and Cd, as well as non-metallic elements such as Si or P [339–351]. It should be stressed that thanks to LVE methodology, it was possible to prepare various Pd alloys in a wide composition range, which would have been much more difficult to obtain by some other methods of preparation.

Influence of alloy formation on the thermodynamics of hydrogen electrosorption

The general shape of H/M vs. potential plots for Pd alloys is similar to that for pure Pd, with the regions of hydrogen adsorption and absorption in the α- and β-phases (for Pd-rich alloys). However, the formation of an alloy modifies the amount of hydrogen absorbed in each phase as compared with Pd. Regarding the influence of alloy bulk composition on the amount of hydrogen electrosorbed at various potentials, three types of regularities were observed (Fig. 6). In the case of Pd–Pt [206, 220, 234, 235] and Pt-rich Pd–Pt–Au [155, 227] alloys, the absorption capacity decreases monotonically with decreasing Pd bulk content for all potentials of hydrogen electrosorption, i.e., for both the α- and β-phases. A different behavior is exhibited by Pd–Au [207, 220, 233, 235] and Au-rich Pd–Pt–Au [155, 227] alloys, where at relatively high potentials the amount of electrosorbed hydrogen increases with decreasing Pd bulk concentration, passes through a maximum, and then decreases. On the other hand, at sufficiently low potentials, where the hydrogen solubility is close to the maximum value, a monotonic decrease in the alloy absorption capacity is observed with decreasing Pd bulk content, similar to the case of the Pd–Pt alloys. An opposite situation takes place for Pd–Rh alloys [154, 239]. In that case, the absorption capacity at higher potential decreases with decreasing Pd bulk content, while at lower potentials it passes through a maximum for Pd bulk content of 90–95%. For these alloy compositions, the maximum ability to absorb hydrogen is higher (H/M >0.80) than that for pure Pd (H/M=0.74).

The above tendencies are in line with the data for hydrogen absorption from the gas phase and can be explained by taking into account the influence of the geometric and electronic effects on hydrogen solubility [3, 119–125, 342–346]. The former effect is related to the changes in the crystal lattice parameters upon Pd alloying with other metals. The latter effect concerns the alteration of Pd *d* band electronic structure due to the electron transfer from the alloying metal.

For Pd-rich alloys, a miscibility gap is present in the phase diagram of the alloy–hydrogen system, as in the case of pure Pd [124, 125]. Typically, with the increase in the amount of alloying metal, the maximum hydrogen content in the α-phase (α_{max}) increases, while the minimum hydrogen content in the β-phase decreases (β_{min}); as a result, the two-phase region is narrowed. This effect corresponds to a decrease in the critical temperature of the Pd alloy–hydrogen system with respect to pure Pd [3]. At a given temperature for a certain alloy bulk composition, the miscibility gap in the alloy–hydrogen system disappears (i.e., $\beta_{min}=\alpha_{max}$) and the β-phase can no longer be formed. In alloys containing less Pd in the bulk, only a single phase of absorbed hydrogen exists and no phase transition occurs. According to Hubkowska et al. [233, 234] and Łukaszewski et al. [235], these limiting bulk concentrations of Pd vary between 75% and 79% in the temperature range 283–313 K for Pd–Au alloys and between 82% and 87% in the temperature range 283–328 K for Pd–Pt alloys. The results obtained in electrochemical experiments are in good agreement with other literature data, according to which the aforementioned limiting alloy compositions (at normal

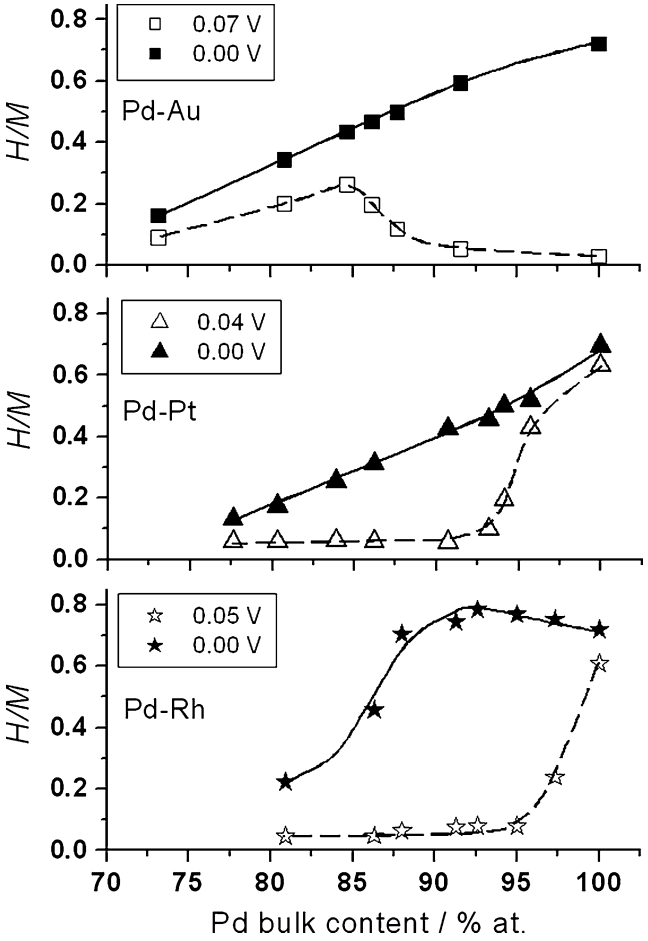

Fig. 6 Influence of alloy bulk composition on the amount of hydrogen absorbed at various potentials (vs. RHE) in Pd alloy LVEs (thickness, 0.7–1.1 μm) at room temperature [235, 239]

conditions) correspond to approx. 70–83% Pd in the bulk for the Pd–Au system [3, 125, 347] and to approx. 82–88% Pd for the Pd–Pt system [3, 124, 348–351]. Only in the case of Pd-rich Pd–Rh alloys does the minimum hydrogen content in the β-phase increase as compared with pure Pd; however, for the alloys containing less Pd, the H/M ratio at the β-phase boundary becomes lower, as for other systems [124, 352].

A strong depletion of Pd in the bulk leads to a further decrease in the alloy absorption capacity. The limiting bulk concentration of the alloying metal for which the alloy's ability to absorb hydrogen ceases is approx. 30% for Pd–Pt alloys [206], 40% for Pd–Pt–Rh alloys [216], 45% for Pd–Rh alloys [154], and 60–70% for Pd–Au [207] and Pd–Pt–Au alloys [155]. For a series of alloys containing less Pd in the bulk, only hydrogen adsorption on the surface is possible.

Grdeń et al. [206] demonstrated that the amount of hydrogen absorbed in Pd alloys is governed almost exclusively by Pd bulk content. For Pd-Pt alloys of a similar bulk composition, the values of H/M ratio differed only by several percentages between samples superficially rich and poor in Pd.

The analysis of the potential range of the phase transition reveals that the alloys investigated exhibit two kinds of behavior. For Pd–Au, Pd–Ag, Pd–Cd, Pd–P, and Au-rich Pd–Pt–Au alloys, the α–β transition occurs at potentials higher than on Pd; moreover, the potential of the phase transition is shifted positively with the decrease in Pd content in the alloy bulk. A different situation is observed for Pd–Ni, Pd–Rh, Pd–Pt, Pd–Pt–Rh, and Pt-rich Pd–Pt–Au alloys, with the potential of the phase transition shifted into a negative direction with respect to the case of pure Pd and decreasing with a decrease in Pd content [154, 155, 206, 207, 216, 222, 226, 227, 231, 233–235, 238, 239]. From the thermodynamic point of view, these results indicate that the β-phase generated electrochemically in Pd–Au, Pd–Ag, Pd–Cd, Pd–P, and Au-rich Pd–Pt–Au systems is more stable than in pure Pd, while for other systems it is less stable [3, 116–118, 298, 299, 301].

The shift of the phase transition region is generally explained by the aforementioned geometric effect connected with the changes in crystal lattice due to alloy formation [3, 119–125, 342–346]. It has been observed that for disordered substitutional face-centered cubic Pd alloys of the lattice parameter higher than in Pd (so-called expanded alloys), the region of α–β phase transition is placed at a lower hydrogen pressure, which corresponds to a higher potential value in an electrochemical experiment. On the contrary, for systems of a smaller lattice parameter than that of Pd, a lower potential is required for the phase transition. Such a behavior is a consequence of the different amounts of work to be done during the α–β transition to extend the lattice in an expanded/contracted system [344]. Exceptionally, despite the crystal lattice expansion after Pd alloying with Pt [124], the Pt–Pd system behaves as a contracted alloy. In that case, a decrease in compressibility due to Pt addition seems to play a more important role here than the geometric factor [351]; the effect of a large broadening of the valence band upon alloying is also reported in the literature [349].

Łukaszewski et al. [222] demonstrated a correlation between the potentials of the α–β phase transition and bulk composition of Pd alloys with Pt, Au, and Rh. Later results by Hubkowska et al. [233, 234] confirmed this tendency also for the potential of the reverse β–α phase transition and for various temperatures (in the range 283–328 K). It was suggested that these correlations could be utilized for the in situ determination of bulk composition of Pd-rich alloys directly from the hydrogen absorption experiment [222, 238].

Similar to the case of pure Pd, a hysteresis in the phase coexistence region was observed for Pd alloys with Au, Ag, Pt, and Rh [154, 155, 216, 226, 233, 234]. The extent of hysteresis for the alloys is generally smaller than for Pd. In the case of alloys sufficiently poor in Pd,

the hysteresis disappears, i.e., the potentials of the α→β and β→α phase transitions become identical. The strongest effect of the metal additives was observed in the case of Pd–Pt alloys, where already approx. 12% of Pt in the bulk was sufficient for hysteresis to be completely reduced [234]. For Pd–Au alloys, the limiting alloy composition was approx. 25% of Au [233], while for Pd–Rh alloys it was above 30% of Rh [154].

From the analysis of the changes in the phase transition potential with temperature, it is possible to calculate the thermodynamic parameters of hydrogen absorption in Pd under electrochemical conditions. Hubkowska et al. [233, 234] determined the values of Gibbs' free energy, enthalpy, and entropy of the processes of the hydride phase formation and decomposition for Pd–Au and Pd–Pt alloys in the form of LVEs (thickness of 0.7–1.1 μm). Although the absolute values of ΔH and ΔS obtained in the electrochemical studies were approx. 30–45% higher than those determined under the gas phase conditions [347, 351], the general trends in the changes of $\Delta H_{\alpha-\beta}$ and $\Delta S_{\alpha-\beta}$ with alloy composition were identical, with similar slopes of the relationships. The discrepancies between both sets of thermodynamic data may be ascribed to the different states of the samples resulting from a different method of preparation, pretreatment, different thicknesses of the hydrogen-absorbing material, and a different procedure of hydrogen absorption. As a result, the samples used by various authors might have been expected to differ with respect to both surface and bulk microstructures, grain size, internal stresses, etc., which could lead to a different thermodynamic behavior. It was demonstrated that the size effect might considerably influence the thermodynamic properties of Pd samples [317, 318, 325].

Influence of alloy formation on the rate of hydrogen electrosorption

The rate of hydrogen absorption and desorption into/from some Pd alloys was found to be higher than in pure Pd. A tendency toward faster hydrogen absorption upon Pd alloying with Au, Ag, Pt, Rh, or Cd was also reported by Liu et al. [148], Łukaszewski et al. [231, 237], Chen et al. [335], Lasia et al. [336], and Adams et al. [337, 338]. It was reported that the time needed for a complete hydrogen saturation or removal (normalized to the amount of electrosorbed hydrogen) tended to decrease with increasing bulk content of the alloying metals. In particular, the maximum absorption/desorption time corresponding to the phase transition potential considerably decreased upon Pd alloying with other noble metals. These effects were accompanied by the increase in hydrogen absorption or desorption currents recorded in chronoamperometric experiments [231, 237].

Another fact indicating facilitated kinetics of hydrogen electrosorption in Pd alloys with Pt, Rh, Au, or Ag was the increased electrochemical reversibility between absorption and desorption. Łukaszewski et al. [155, 222, 230, 231, 237] found a correlation between the potential of the main peak due to hydrogen oxidation and alloy bulk composition. The value of peak potential decreased almost linearly with increasing amounts of the alloying metals, with the strongest effect of Pt additive. Hubkowska et al. [233, 234] confirmed this correlation for Pd–Au and Pd–Pt alloys at different temperatures (283–328 K). The tendency toward the easier oxidation of absorbed hydrogen was observed for various Pd alloys, regardless of the changes in the thermodynamic stability of the β-phase indicating the kinetic origin of that effect. The possible reasons may be the acceleration of surface steps of hydrogen electrosorption in the presence of other noble metals or the faster phase transition due to the reduction of the hysteresis effect. Thus, it was concluded that some metals not absorbing hydrogen in their pure state when added to Pd might considerably improve the kinetics of hydrogen absorption/desorption processes, although the maximum of absorbed hydrogen is usually reduced in those alloys in comparison with Pd [231, 237].

Mechanism and kinetics of hydrogen electrosorption in LVEs

General scheme of hydrogen electrosorption

On the basis of the literature data [4, 47, 127, 171, 177, 191, 193, 195, 198, 202, 203, 207, 208, 212, 220, 224, 237, 258, 259, 262, 265, 267–269, 271, 273, 288, 293, 348, 353–366], the possible interactions of hydrogen with a Pd-based electrode during the electrosorption process can be summarized in the following scheme[1] (for acidic solution):

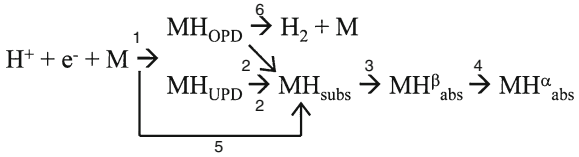

The particular steps of hydrogen electrosorption are:

1. Volmer reaction, i.e., charge transfer followed by the adsorption of H atoms on surface active sites (hollow site for UPD H or on-top position for OPD H);

[1] The order of the phases of absorbed hydrogen in the scheme follows the hydrogen concentration profile across the electrode according to a model postulated in the literature [293]. Therefore, the β-phase precedes the α-phase. During hydrogen sorption, the α→β phase transition takes place with the phase boundary, moving from the surface to the electrode interior.

2. Transfer of atomic hydrogen (UPD H or OPD H) from the surface through the interface to an interstitial position in a subsurface layer (H_{subs});
3. Diffusion of hydrogen from the subsurface layer to the bulk of the metal, where a particular phase of absorbed hydrogen is formed;
4. Phase transition between the α- and β-phases of absorbed hydrogen;
5. Charge transfer followed by the transfer of atomic hydrogen to an interstitial position in a subsurface layer, without the adsorption step (direct absorption); and
6. Discharge of adsorbed H atoms (only OPD H) in an electrochemical process (Heyrovsky reaction) or a chemical recombination process of H atoms (Tafel reaction), both leading to the hydrogen evolution reaction.

According to the above scheme, the two main mechanisms of hydrogen absorption can be considered, namely, the so-called indirect absorption path and the direct absorption path. These mechanisms differ with respect to the participation of hydrogen adsorbed on the surface in the process of hydrogen transfer from solution to the subsurface layer.

In the scheme above, it was shown that hydrogen electrosorption in Pd-based LVEs is a complex reaction consisting of several steps or parallel paths. Depending on experimental conditions, different steps may be rate-limiting for the overall electrosorption process (or even a mixed control can occur), i.e., hydrogen diffusion in the bulk, hydrogen transfer through the interface, the α–β phase transition, or the surface electrochemical reaction. Additionally, different steps can be influenced by the electrode potential and temperature or alloy composition in a different manner. Thus, to study the kinetics of a particular absorption step, the experimental conditions should be adjusted so that the process investigated is the slowest step in the reaction sequence.

The role of phase transition

Phase transition is an important step of hydrogen absorption or desorption into/from Pd-based electrodes. Two mechanisms of phase transition were considered, namely, nucleation and growth mechanism [367, 368] or moving phase boundary mechanism [288, 293, 297]. The latter mechanism is strongly supported by the results reported by Skorodumov et al. [369]. According to this picture, during the coexistence of both phases of absorbed hydrogen, there is a movement of a sharp α–β phase boundary inside the metal, leading to a discontinuous hydrogen concentration gradient [288, 293, 297].

In a model developed by Choi et al. [370], and Lee and Pyun [293] for the insertion/extraction of ionic species into/from the metal host lattice, in the phase coexistence, the composition of the outermost layers is different from that of the bulk. For instance, in the absorption process at potentials low enough for the β-phase to be formed, after a rapid initial formation of the α-phase, the β-phase appears in the subsurface region with a phase boundary moving from the surface to the bulk of the electrode. According to Choi et al. [370], during potential jumps across the phase transition region, the driving force for the current is the potential difference between hydrogen saturation/extraction potential and the phase transition potential. Simultaneously, the time for a complete phase transition is proportional to the transferred charge and inversely proportional to the aforementioned potential difference.

From the data on the influence of electrode potential on the time needed for a complete hydrogen saturation and removal as well as from the analysis of chronoamperometric curves recorded during hydrogen absorption and desorption, Łukaszewski et al. [216] concluded that in the presence of both the α- and β-phases of absorbed hydrogen, the slow process of the phase transition controlled the rate of the overall reaction of hydrogen electrosorption in Pd-based LVEs. This interpretation was in line with some other authors' suggestions made earlier for pure Pd [288, 297, 371]. In particular, the influence of the rate of the α–β phase transition on the measured hydrogen current was demonstrated by Zhang et al. [288] by theoretical modeling of CV curves for a thin Pd electrode. The characteristic shape of hydrogen signals and a significant separation between the cathodic and anodic peaks was explained assuming the α→β and β→α phase transitions as the slowest steps in the overall electrosorption process in thin Pd layers. These findings were confirmed for Pd alloys with Au, Rh, Pt, Ag, Cu, and Cd [154, 155, 216, 232, 235, 237, 335, 338]

Łukaszewski et al. [237] demonstrated a correlation between the rate of hydrogen electrosorption and the extent of hysteresis for Pd alloys. It was also proven by normalizing the kinetic parameters with respect to the amount of electrosorbed hydrogen that the increased rate of hydrogen electrosorption in the alloys did not result simply from the lower amount of absorbed hydrogen in comparison with pure Pd [231, 235]. It was suggested that Pd alloying with such metals as Rh, Ag, Pt, and Au could facilitate the process of hydrogen electrosorption, with the influence on the rate of the phase transition as one of the key factors [237].

Mechanism of hydrogen desorption from Pd LVEs

During the desorption process, hydrogen can also leave the metal directly or via the adsorption step. It was demonstrated that the indirect hydrogen desorption can proceed via two paths, namely, the electrochemical oxidation and

the non-electrochemical recombination of hydrogen atoms [193, 202, 203, 208].

A key argument for the validity of this mechanism was the characteristic dependence of the hydrogen oxidation charge on the scan rate in a cyclic voltammetric experiment. The amount of hydrogen electrooxidized at the slowest scan rates (below 0.005 Vs^{-1}) was 10–20% lower than the maximum amount measured at faster scan rates [202, 203, 208]. Under these conditions, more hydrogen is removed via the recombination process, which decreases the amount of hydrogen desorbing via the charge transfer process [202, 203, 208]. At higher scan rates, the sufficiently high potentials for hydrogen electrooxidation are reached faster and the ratio of the rate of electrooxidation to the rate of recombination rises, which is reflected in the increase in the hydrogen oxidation charge in a certain range of scan rates. Maximum charge due to hydrogen oxidation corresponds to scan rates in the range 0.01–0.02 Vs^{-1}. At these scan rates, all absorbed hydrogen leaves the electrode via an electrooxidation process. For faster polarization, again, a decrease in hydrogen oxidation charge was observed, which could be explained by the fact that due to diffusional limitations, not all hydrogen was transferred from the bulk to the surface during one fast anodic scan [202, 203, 208].

The results reported for Pd–Au, Pd–Pt, Pd–Rh, Pd–Ag, Pd–Cu, and Pd–Pt–Rh alloys [156, 207, 212, 224, 237] show that such a behavior of absorbed hydrogen does not have to be exclusively the characteristic of pure Pd, but it may be a more general phenomenon typical of Pd-based absorbing systems. A comparison of the maximum effect of the lowering of hydrogen oxidation charge for Pd and its alloys [237] revealed that the greatest relative decrease in hydrogen oxidation charge (up to 20%) was observed for Pd, Pd–Pt, and Pd–Pt–Rh alloys, while the smallest effect (below 7%) was visible for Pd–Au, Pd–Cu, and Pd–Ag alloys.

The experiments with CO_2 adsorption on Pd alloys performed by Grdeń et al. [205], Łukaszewski et al. [64, 65, 210, 213], and Siwek et al. [66, 214] proved that the electrochemical absorption and desorption of hydrogen into/from homogeneous Pd–Pt, Pd–Rh, and Pd–Pt–Rh alloys proceed exclusively via Pd surface sites. However, a strong decrease in hydrogen oxidation charge at low scan rates for Pd–Pt and Pd–Pt–Rh alloys suggests that for Pd alloys with metals which are able to adsorb hydrogen, the non-electrochemical recombination reaction can proceed between all the surface sites which are accessible for hydrogen, namely, both Pd–Pd neighboring centers and Pd–Pt or Pd–Rh centers [212, 237]. On the other hand, a much smaller contribution of the non-electrochemical desorption for Pd alloys with such metals as Au, Cu, or Ag can be explained by their inertness in hydrogen electrosorption above the potentials of hydrogen evolution [156, 237]. These conclusions were confirmed in the experiments performed with Pd–Au alloys of different surface compositions [156]. For alloys superficially impoverished with Pd, the importance of the recombination reaction was smaller than for alloys rich in Pd on the surface.

The effect of the decrease in hydrogen oxidation charge was not just limited to the high electrode saturation with hydrogen in the β-phase region but was also observed for lower amounts of absorbed hydrogen, corresponding to a mixture of the α- and β-phases or even to the pure α-phase [212]. Therefore, it was concluded that the dual mechanism of hydrogen desorption might not be strictly connected with a particular phase of absorbed hydrogen. The effect was still observed even for potentials considerably higher than the reversible potential of hydrogen evolution reaction, suggesting that the full surface coverage with adsorbed hydrogen is not a requisite condition for that phenomenon. However, it remains unclear whether both OPD H and UPD H can participate in the recombination process of adsorbed hydrogen atoms generated on the surface of Pd-based electrodes from absorbed hydrogen during the desorption process.

It should be noted that absorbed hydrogen in palladium has a strong tendency to leave the metal without any anodic electrochemical polarization. Schuldiner et al. [372] and Rosamilia et al. [186] reported that at the open circuit potential electrosorbed hydrogen diffuses spontaneously out of the fully saturated bulk palladium. This effect is caused by a low partial pressure (close to zero) of hydrogen dissolved in the solution, which shifts the equilibrium between absorbed, adsorbed, and gaseous hydrogen in the direction of desorption. Traces of oxygen present in the solution may also affect this process.

The role of subsurface hydrogen

Subsurface hydrogen is an intermediate form between hydrogen existing outside the metal and that dissolved in the metal bulk. The formation of a subsurface layer of sorbed hydrogen has been postulated by Breiter [366] as the first step of hydrogen incorporation into palladium during the absorption process. Also, Yoshitake et al. [373] claimed that the exchange reaction occurs between hydrogen on the palladium surface and deuterium from the subsurface. Conway and Jerkiewicz [362], and Jerkiewicz and Zolfaghari [171], in their models of cathodic hydrogen sorption, postulated that before the formation of the bulk phases of absorbed hydrogen some kind of equilibrium occurs between the adsorbed and subsurface states of hydrogen. However, in the literature, there is a controversy whether the existence of subsurface hydrogen is limited to the first metal layer just beneath the surface or it can be treated as a separate phase of hydrogen dissolved in a layer of a certain thickness.

According to Bucur and Bota [360], the concentration of hydrogen dissolved in the subsurface layers exceeds its concentration in the bulk of Pd. Thus, the existence of subsurface hydrogen could explain the increase in H/Pd ratio with decreasing thickness of Pd LVEs. In a model of hydrogen electrooxidation from a Pd electrode, Bucur and Bota [360] proposed that hydrogen dissolved in the first several layers (of thickness approx. 20–50 nm) of the metal (subsurface hydrogen) plays an important role during electrooxidation. Adapting this idea, Czerwiński et al. [202, 203] postulated that the subsurface layer of hydrogen could exist not only during hydrogen sorption but also during the opposite process, i.e., hydrogen desorption from the metal, when hydrogen present in the subsurface layer is responsible for the generation of hydrogen sorbed on the surface of Pd LVEs. The analysis of the influence of scan rate and electrode thickness on hydrogen oxidation charge strongly suggested the existence of the subsurface hydrogen, which probably is crucial in the hydrogen removal process, especially for thin Pd layers.

In the above model of hydrogen desorption from Pd LVEs during the first step of desorption, hydrogen diffuses to the subsurface layer, where it is in equilibrium with the adsorbed hydrogen at the Pd surface, and finally is removed from the electrode by electrooxidation or chemical recombination. Other forms of hydrogen, i.e., the α- and β-phases, contribute indirectly (by supplying the subsurface layer) to the measured hydrogen oxidation charge [202, 203].

In alkaline solutions, the influence of alkali metal cations on the process of hydrogen electrosorption was observed [127, 128, 194, 196, 199, 200, 203, 208]. The values of the electrochemically measured H/M ratio and their dependence on electrode thickness and scan rate in voltammetric experiments were affected by the kind of alkali metal cation present in the solution [203]. This effect was interpreted in terms of the different interactions between various alkali metals and hydrogen in the subsurface layer. The experiments with the flow-through Pd electrode confirmed that lithium was introduced irreversibly into palladium during hydrogen electrolysis from 0.1 M LiOH [203]. The results of Yamazaki et al. [374] showed that maximum Li concentration in a Pd electrode was reached at a depth of approx. 25 nm below the surface. According to Czerwiński et al. [203], the concentration of lithium and other alkali metals in the subsurface layer of the palladium electrode is significantly higher than in the bulk of the metal. These metals inside Pd probably generate hydrides which are in equilibrium with all forms of absorbed hydrogen, affecting the process of its absorption and subsequent desorption. The interactions of the incorporated metal with absorbed hydrogen and Pd can stabilize the system by constituting ternary alloys, like Pd–Li–H or Pt–Rb–H [375, 376]. Since the surface layer of alkali metals incorporated should be thermodynamically unstable in contact with water, their dissolution might generate concentration profiles where the concentration of the alkali metal is depleted near the surface, as reported by Yamazaki et al. [374]. The exact profile of the alkali metal concentration in the subsurface layer affects the rate of hydrogen diffusion from the bulk of the metal toward the surface of a Pd electrode. Probably, due to the presence of alkali metal in Pd, the subsurface layer of hydrogen in basic solutions is thinner than that in acidic solutions. Incorporated alkali metals enhance also the isotopic effect observed for hydrogen and deuterium absorption form basic solutions [203].

In contrast to pure Pd, the possibility of the existence of subsurface hydrogen still awaits verification in the case of Pd alloys. It was suggested that such phase might be present for alloys sufficiently rich in Pd and play an important role in the process of hydrogen removal [212]. However, the results reported by Żurowski et al. [224] did not reveal the influence of the electrode thickness (in the range 0.11–1.55 μm) on the amount of hydrogen absorbed in Pd–Rh alloys (84–87% Pd in the bulk). Therefore, it was concluded that the behavior of hydrogen absorbed in Pd–Rh alloys was different from that in pure Pd alloys and that the layer of subsurface hydrogen was not formed or at least was much less developed, i.e., thinner or poorer in hydrogen than in Pd. Taking into account that Pd-rich Pd–Rh alloys can absorb more hydrogen than pure Pd, it may also be supposed that the high concentration of hydrogen in the alloy bulk is more uniform than in Pd, and therefore, the separate phase of subsurface hydrogen is much less pronounced. In that context, it should be mentioned that there were suggestions that hydrogen absorbed in Pd–Rh alloys is located preferentially around Rh, not Pd atoms [123]. Thus, Rh addition to Pd might change the distribution of hydrogen in the alloy in comparison with pure Pd.

Hydrogen diffusion in Pd LVEs

Due to a small thickness of LVEs, hydrogen diffusion in the bulk of the metal is not usually expected to be the slowest step of the overall hydrogen electrosorption process. However, at sufficiently high/low potentials of hydrogen absorption/desorption, at fast scan rates, in the absence of a slow phase transition or for relatively thick layers, diffusional limitations can be observed in electrochemical experiments. Various electrochemical techniques used for studying hydrogen diffusion in metals, like transient, potentiodynamic, and ac–av techniques, have been reviewed by Pound [4], Züchner and Boes [377], as well as Zoltowski [294]. The analysis of the electrochemical response under diffusion-controlled conditions of hydrogen oxidation can be found in the literature [291, 293, 378, 379].

Examples of literature data on hydrogen diffusion parameters for thin Pd-based electrodes are shown in Table 1. The

Table 1 Hydrogen diffusion coefficients (at room temperature) determined electrochemically in thin Pd-based electrodes

Reference	Electrode material	Solution	Method	Electrode thickness (μm)	D_H ($cm^2\ s^{-1}$)	
					α-phase	β-phase
[297]	Pd foil	1 M H_2SO_4	CA, EIS	47	3×10^{-7}	1×10^{-6}
[247]	Pd evaporated on Au-coated Ni	6 M KOH	CA	0.046	2.1×10^{-11}	
				0.135	3.0×10^{-10}	
				25	1.6×10^{-7}	
[382]	Pd–Pt (86% Pd) electrodeposit	0.5 M H_2SO_4	CA	1.5–8.1	9.5×10^{-8}	
[237]	Pd electrodeposit	0.5 M H_2SO_4	CA	0.4–0.8	1×10^{-7}	
	Pd–Rh (68–100% Pd) electrodeposit			0.4–0.8	1×10^{-7}–1×10^{-8}	
	Pd–Ag (88–100% Pd) electrodeposit			0.4–0.8	1×10^{-7}–5×10^{-8}	
	Pd–Cu (75–100% Pd) electrodeposit			0.4–0.8	1×10^{-7}–2×10^{-8}	
	Pd–Pt–Au (80–100% Pd) electrodeposit			0.9–1.5	1×10^{-7}–4×10^{-8}	
[334]	Pd disc	1 M H_2SO_4	CA, EIS	50	3×10^{-7}	
	Pd–Pt (81% Pd) disc			50	1.2×10^{-7}–5×10^{-8}	
[308]	Pd–Pt (81% Pd) foil	0.1 M H_2SO_4	Permeation, EIS	50	1.2×10^{-7}–7×10^{-8}	
[383]	Pd–Rh (79.5% Pd) sheet	0.6 M K_2CO_3	CA	150	1×10^{-7}	
		0.5 M LiOH			1×10^{-7}–4×10^{-8}	
[341]	Amorphous Pd–Ni–Si (82–50% Pd, 18% Si) ribbon	0.1 M NaOH	CA	30	1.3×10^{-8}	

values of hydrogen diffusion coefficient in Pd alloys with such metals as Au, Ag, Cu, Pt, Rh, and Ni are smaller than those for pure Pd despite different trends in changes in the lattice parameter upon Pd alloying with those metals. Thus, the alteration of the volume of the octahedral void accessible for hydrogen is not the only parameter influencing the rate of hydrogen diffusion in Pd alloys [380, 381]. Moreover, in light of the improved kinetics of hydrogen absorption/desorption into/from Pd alloys with Pt, Au, Rh, and Ag, the fact that the values of D_H in the alloys are lower than in Pd confirms that diffusion itself is not a decisive factor determining the rate of the oxidation of hydrogen absorbed in thin Pd-based films [237].

The role of alloy composition and distribution of different metal atoms in the crystal lattice on hydrogen diffusion in Pd-based fcc alloys was studied by Opara et al. [384] and Barlag et al. [385]. They calculated the values of D_H applying the method of Monte Carlo simulation assuming a simple model of a roundabout way diffusion based on the assumption of at least two different jump frequencies of the hydrogen atoms when moving from one interstitial site to a neighboring one, caused by the two types of octahedrals differing from each other by their direct environment, according to the kind of the surrounding metal atoms, i.e., the sites formed by predominantly Pd atoms and those with the neighborhood of more than two atoms of the alloying metal. For the Pd–Ag system, the authors found that at smaller Ag contents, the Ag atoms partly block the energetically favored diffusion paths in the Pd matrix, while at high Ag concentrations, Pd atoms act as traps for hydrogen in a silver matrix. The interplay of the hydrogen transport via two kinds of occupation sites with different hydrogen solubilities determines the shape of the curve for the macroscopic diffusion coefficient as a function of the alloy composition.

Simultaneous examination of hydrogen electrosorption and other phenomena with the use of LVEs

As stated in "Idea of LVEs," LVEs enable studying simultaneously both bulk and surface reactions proceeding in/on Pd-based materials. Below, selected examples will be given of the investigations that were possible due to the unique advantages of the LVE methodology.

Separation of hydrogen adsorption and absorption

Due to the fact that potential ranges of hydrogen adsorption on and absorption in Pd are overlapped, the separation between the contributions from both these processes was usually a problem. The earlier methods of extracting the contribution from hydrogen adsorption were based on the fact that adsorption is much faster than absorption. Thus, by extrapolating the measured hydrogen charged to zero time of an experiment (e.g., to infinite charging rate in the galvanostatic method or infinite scan rate in cyclic voltammetry), it was possible

to determine the amount of adsorbed hydrogen [45]. However, the use of LVEs for electrochemical studies on Pd has created new possibilities to distinguish hydrogen adsorption and absorption.

As demonstrated by Baldauf and Kolb [92] for ultrathin Pd layers (below three monolayers), hydrogen absorption does not occur, so the electrochemical signal recorded originates from the adsorption alone. The ability of Pd to absorb hydrogen absorption starts at a thickness of three atomic layers. For such thin electrodes, the voltammetric peaks due to hydrogen absorption are well separated from the signals due to hydrogen adsorption. However, in the case of Pd sub-monolayers or several monolayers, a significant influence of the deposit matrix on the voltammetric profile was observed [174, 175, 189, 190, 270, 272–274]. With the increase in Pd layer thickness, the latter effect disappeared [126–128, 192], but the currents originating from adsorption and absorption become more overlapped, with usually more complicated CV profiles, especially in the case of Pd alloys [206, 213, 216, 217]. However, as demonstrated by Grdeń et al. [206] and Łukaszewski et al. [220], although none of the signals on a CV curve can be unequivocally attributed to the oxidation of exclusively one form of electrosorbed hydrogen, it is still possible to indicate processes giving a dominant contribution to each signal. Such a distinction can also be made with the help of certain surface poisons which adsorb on the electrode surface and influence the processes of hydrogen adsorption and absorption in a different manner [210, 211, 213]. Podlovchenko et al. [245], using electrodeposits of Pd on Pt, demonstrated a method utilizing Cu UPD for distinguishing between adsorbed and absorbed hydrogen. By suppressing hydrogen adsorption by foreign metal adatoms, they could determine the solubility of hydrogen in the α-phase alone.

Gabrielli et al. [263], Martin and Lasia [270], as well as Duncan and Lasia [272] elaborated a procedure for the determination of hydrogen adsorption isotherm on a Pd electrode utilizing the LVE methodology. They found a linear dependence of the total hydrogen charge on the electrode thickness in the potential range of the α-phase existence. By the extrapolation of the total amount of sorbed hydrogen to zero thickness, the amount of hydrogen adsorbed at a given potential can be extracted. However, this method could not be applied for lower electrosorption potentials, i.e., in the presence of the β-phase, where due to a much greater contribution from hydrogen absorption, the inaccuracy of the determination of the small amount of adsorbed hydrogen became too high. According to the dependence of the amount of adsorbed of hydrogen on the electrode potential obtained by the aforementioned procedure for a Pd electrode, at potentials close to the α–β phase transition potential, the surface coverage with adsorbed hydrogen reaches approx. 0.76, i.e., below a monolayer.

The above method was used by Żurowski et al. [224] to determine surface coverage with hydrogen adsorbed on Pd–Rh alloys (84–87% Pd in the bulk). Again, the amount of adsorbed hydrogen did not reach a monolayer even at potentials of the β-phase formation. From the comparison with analogous data for pure Pd, it was concluded that hydrogen adsorption on Pd–Rh alloys was weaker. This finding, together with an increased absorption capacity, was believed to support the hypothesis on a significant direct hydrogen absorption/desorption path in the case of Pd–Rh alloys.

Adsorption of surface poisons and their influence on hydrogen sorption

It is known that the presence of some adsorbates influences the processes of hydrogen electrosorption on platinum group metal electrodes [4, 386–389]. In the case of Pd-based LVEs, the effect of such surface poisons as crystal violet [92, 259, 268, 271–273, 339], benzotriazole (BTA) [269], CO_2 [64–67, 205, 210, 213–215, 218, 228], or CO [64–67, 192, 193, 195, 198, 210, 211, 215, 218, 224, 237, 266] on hydrogen adsorption/absorption/desorption was studied.

Baldauf and Kolb [92] investigated the influence of crystal violet adsorption on hydrogen electrosorption in ultrathin Pd layers in acidic solutions. These studies were continued by Bartlett and Marwan [259], Birry and Lasia [268], and Duncan and Lasia [271–273] for Pd as well as Słojewski et al. for Pd–P alloys [339]. It was observed that in the hydrogen adsorption region, currents were strongly suppressed due to crystal violet adsorption, while the process of absorption became electrochemically more reversible. Impedance data showed that in the presence of crystal violet, the charge transfer resistance decreased [271]. It was concluded that crystal violet adsorption inhibited hydrogen adsorption, but the kinetics of hydrogen absorption was significantly enhanced. In the presence of crystal violet, more hydrogen was absorbed in the α-phase, while in the β-phase the amount of absorbed hydrogen as well as the potential of the phase transition remained almost unchanged [272]. Similar tendencies of the changes in hydrogen adsorption and absorption currents were observed by Martin and Lasia [269] in the presence of adsorbed BTA on Pd in alkaline solutions. Bartlett and Marwan [259] found that a sub-monolayer of Pt atoms also blocks the formation of adsorbed hydrogen, but enhances the rate of hydrogen absorption. Muralidharan et al. [390] reported that hydrogen absorption in Pd was facilitated in the presence of lignin. In that context, it should be mentioned that the entry of hydrogen into metals is also promoted by

the so-called hydrogen entry promoters, i.e., the compounds involving such elements as P, As, Sb, S, Se, and Te [4].

The selective effect of the adsorbates like crystal violet or BTA was explained taking into account the direct mechanism of hydrogen absorption. According to Bartlett and Marwan [259], the strongly adsorbed UPD hydrogen acts as a barrier to the absorption of hydrogen into the metal. Birry and Lasia [268], as well as Duncan and Lasia [271–273], also suggested that a fast direct hydrogen absorption mechanism proceeds in parallel with a slower hydrogen adsorption and an indirect absorption. Martin and Lasia [269] noted that in the case of the indirect mechanism, the chemical potentials of adsorbed and absorbed hydrogen should be equal, and therefore the amount of hydrogen in the bulk would be determined by the amount of hydrogen on the surface. In such a situation, strong blocking of hydrogen adsorption would lead to a weaker absorption, which was not observed experimentally, supporting the mechanism of a direct absorption.

Carbon monoxide is known as a strong surface poison inhibiting electrocatalytic processes. In particular, the presence of CO has a great blocking effect on the process of hydrogen electrosorption on all platinum metals [391–393]. In a series of experiments with CO adsorption on Pd-based LVEs [64, 65, 67, 192, 193, 195, 198, 207, 210, 211, 215, 218, 224, 237], the influence of the presence of previously adsorbed CO layer on hydrogen insertion into the electrode and the influence of the presence of adsorbed CO layer on the removal of previously absorbed hydrogen were examined.

Czerwiński's group found that the presence of the products of CO adsorption on the electrode surface strongly influenced both hydrogen adsorption and absorption signals. Under cyclic voltammetric conditions, hydrogen currents were almost totally blocked in comparison with the situation on a clean electrode [64, 65, 67, 192, 193, 195, 198, 207, 210, 211, 215, 218, 224, 237]. Due to high surface coverage with adsorbed CO, very few surface sites remained available for hydrogen atoms. Nevertheless, hydrogen insertion into a CO-covered electrode could occur, although this process was much slower and less effective than on a CO-free electrode. The slow hydrogen absorption in a CO-covered electrode suggested that in the presence of adsorbed CO, the generation of a precursor state for absorbed hydrogen, i.e., adsorbed hydrogen, was the slowest step in the overall absorption process [210, 211].

Adsorbed CO also strongly blocks hydrogen removal from the metal in acidic solutions. The effect of trapping of hydrogen previously absorbed in Pd has been observed for a CO-covered electrode, where the voltammetric signal due to hydrogen oxidation was shifted into higher potentials by more than 0.5 V as compared with a clean electrode [192, 193, 195]. However, it was observed that although the oxidation of absorbed hydrogen on a CO-covered electrode was significantly inhibited, hydrogen was always desorbed before the total removal of adsorbed CO. The fact that both absorption and desorption could still proceed even when usual hydrogen adsorption sites were blocked by adsorbed CO was explained assuming that a certain amount of hydrogen might enter the alloy lattice directly, i.e., without an adsorption stage [192, 193].

It was found that part of the absorbed hydrogen could still remain in CO-poisoned Pd after electrode leaving at open circuit for 1 h or even keeping outside the solution in the argon atmosphere for 1 h or for a longer time. After such treatment, the amount of hydrogen present inside Pd corresponded to a H/Pd ratio of approx. 0.40. It was concluded that only some amount of hydrogen could diffuse out of the electrode, while a significant amount was irreversibly blocked in the electrode bulk [193].

In contrast to acidic solutions, in basic solutions, adsorbed CO only blocks hydrogen absorption without an effect on hydrogen desorption. It was suggested that the interactions between absorbed hydrogen and alkali metals inside Pd could account for that behavior [198]. It was proposed that hydrogen atoms absorbed from acidic and basic solutions might be bound in Pd in a different manner, depending on the absence or presence of the aforementioned interactions of hydrogen with alkali metals.

Similar results were reported by Łosiewicz et al. [266] who concluded on the basis of voltammetric and impedance data that hydrogen adsorption did not occur in the presence of adsorbed CO on Pd, while the current during potentiostatic charging in the absorption potential region was very small accompanied by a high charge transfer resistance. The possibility of slow residual hydrogen absorption was attributed to the fact that either the coverage with adsorbed CO was not complete or the CO layer was permeable for hydrogen.

The above observations were confirmed by Łukaszewski et al. for Pd alloys with Au, Pt, and Rh [64–67, 207, 210, 211, 218, 237]. The extent of hydrogen electrosorption blocking by adsorbed CO was dependent on the alloy composition and the related structure of CO adsorption products. In particular, in the case of a Pd–Rh alloy of a moderate Pd bulk content (80%), the effect of adsorbed CO on absorbed hydrogen removal was markedly weaker than for Pd and other alloys, and a certain portion of the absorbed hydrogen could be desorbed without inhibition, indicating the possibility of a greater importance of the direct desorption path for this alloy constitution [224, 237].

Another surface poison affecting hydrogen electrosorption is the adsorption product of CO_2 reduction [228, 394]. On Pt and Rh electrodes at potentials positive to the

reversible hydrogen potential, a reaction between CO_2 molecules and atoms of underpotentially deposited hydrogen takes place, the reduction product becoming adsorbed. Although pure Pd is inactive in the process of CO_2 reduction at potentials of H UPD region [195], CO_2 can be reduced on Pt or Rh surface atoms in their alloys with Pd [64–67, 205, 210, 213–215, 218, 228]. Thus, the influence of this adsorbate on hydrogen electrosorption in Pd alloys with Pt or Rh can be examined.

Grdeń et al. [205] investigated CO_2 reduction on Pd–Pt LVEs, while Łukaszewski et al. [64, 65, 67, 210, 213, 218] and Siwek et al. [66, 214] continued such experiments for Pd–Rh and Pd–Pt–Rh alloys. These studies showed that the different adsorption properties of Pt/Rh and Pd atoms toward CO_2 were retained in the alloy, i.e., in the presence of reduced CO_2, only hydrogen adsorption was partially suppressed while hydrogen absorption remained practically undisturbed. Thus, in a CO_2 reduction experiment performed on Pd alloy LVEs, it was possible to block hydrogen bonded to Pt or Rh surface atoms without any significant effect on hydrogen bonded to Pd atoms. The presence of reduced CO_2 on the electrode surface did not create a significant barrier for both hydrogen insertion and removal into/from the alloy bulk. In contrast to the case of CO adsorption, the effect of reduced CO_2 on the processes of hydrogen absorption/desorption was independent of the fact whether hydrogen was absorbed in an electrode previously covered with the carbonaceous adsorbate or the adsorbate layer was generated after hydrogen saturation.

Grdeń et al. [205] concluded that only Pd surface atoms are active in the processes of the indirect electrochemical absorption and desorption of hydrogen into/from Pd alloys. Hydrogen interacting with Pd surface atoms, which is a precursor state in the hydrogen absorption according to the indirect mechanism, does not participate in the CO_2 reduction reaction. Due to the selective effect of reduced CO_2 on various forms of hydrogen electrosorbed on different metals in a CO_2 adsorption experiment, it was possible to distinguish between signals originating mainly from hydrogen absorption and those with significant contributions from hydrogen adsorption. Łukaszewski et al. [213] demonstrated the possibility of using reduced CO_2 as a kind of diagnostic tool for studying the processes of hydrogen electrosorption in a multi-component Pd alloy (Pd–Pt–Rh), where applying CO_2 reduction allowed for the examination of the nature of multiple hydrogen signals observed in cyclic voltammetric experiments. An effect very similar to that of reduced CO_2, i.e., partial blocking of hydrogen adsorption without blocking hydrogen absorption, was observed by Soszko et al. [72] in the presence of adsorbed methanol on Pd–Pt–Rh alloys.

The interactions of Pd alloy LVEs with hydrogen in the presence of adsorbed CO and reduced CO_2 were summarized in the following schemes [64, 205, 395]:

$$\mathrm{Pd/Pt/Rh} \xrightarrow[CO_2]{H^+ + e^-} \mathrm{Pd\text{–}}\underset{\underset{H_{abs}\ \text{(easy indirect absorption)}}{\uparrow\downarrow}}{H_{ads}} + \mathrm{Pt/Rh\text{–}`CO_2'}$$

$$\mathrm{Pd/Pt/Rh} \xrightarrow[CO]{H^+ + e^-} \underset{\underset{H_{abs}\ \text{(weak direct absorption)}}{\downarrow\uparrow}}{\mathrm{Pd/Pt/Rh\text{–}`CO'}}$$

where "CO_2" and "CO" denote the products of CO_2 and CO adsorption, respectively.

Influence of hydrogen sorption on surface oxidation of metals

In most investigations on the electrochemistry of Pd and its alloys, hydrogen-related phenomena were usually treated separately from the electrode behavior in the region of surface oxidation, and relatively few papers were devoted to the interrelation between the hydrogen absorption process and electrode properties in the potential region where most electrocatalytic processes take place. There were suggestions that some catalytic properties of Pd were different and metal dissolution was suppressed for Pd deposited in the presence of absorbing hydrogen [251, 257, 396]. Other reports indicated that in the presence of absorbed hydrogen in Pd-based electrodes, the oxidation of carbonaceous adsorbates like CO, methanol, and formate ions is facilitated [63, 71, 98].

Using Pd-based LVEs, Łukaszewski et al. [155, 225] compared the electrochemical oxidation of freshly deposited Pd and its alloys with other noble metals (Au, Pt, Rh) with the behavior of samples subjected to prior hydrogen absorption/desorption procedure, demonstrating a significant influence of the electrode hydrogen treatment on the electrochemical properties of surface oxides. It was found that surface oxidation of previously hydrided Pd, Pd–Au, and Pd–Pt–Au deposits could start at lower potentials than on freshly deposited electrodes and was accompanied by a negative shift of the potential of the surface oxide reduction peak [155, 209, 225]. It has been found that this effect occurred even when the freshly prepared electrode had once been polarized into the hydrogen region, and the greatest changes in the peak potential were observed after the first hydriding.

The maximum values of the negative shift of peak potential reached approx. 50 mV for pure Pd, 130 mV for Pd–Au alloys with approx. 70% Pd in the bulk, and even 230 mV for a Pd–Pt–Au alloy with approx. 40% Pd in the bulk [155, 209, 225]. In the latter case, surface oxidation of a Pd–Pt–Rh electrode after hydrogen treatment began at a potential lower than on pure Pt electrode. Since the

electrode ability for surface oxide formation (oxygen adsorption) is crucial for organic fuel oxidation [397], this phenomenon might be promising for the improvement in methanol or ethanol fuel cells.

The increase in the electrochemical stability of surface oxides on hydrogen-treated samples was tentatively related to the changes in alloy crystal lattice during its penetration by hydrogen [209]. However, further studies indicated that full electrode saturation with hydrogen absorbed in the β-phase was not necessary for this phenomenon to occur [155]. The reason for this effect seems to be more subtle, and it might be caused by the alloy interactions mainly with hydrogen present on the surface or in the subsurface region of the electrode.

Another effect of previous hydrogen electrosorption on surface oxidation of Pd-based LVEs concerns electrochemical dissolution of the electrode material. Łukaszewski et al. [225], using EQCM, determined the amount of metals dissolved during electrode polarization in the oxygen region before and after hydrogen treatment. It was found that Pd and its alloys with Au, Pt, and Rh subjected to hydrogen absorption were more resistant to electrochemical dissolution than freshly deposited samples. The enhanced resistance to dissolution of hydrogen-treated samples did not simply result from changes in real surface area since the amount of dissolved metal was normalized per area unit, not from the changes in alloy surface composition, as it occurred not only for alloys but also for pure Pd [225]. The lowering of the dissolution of hydrogen-treated Pd-based electrodes was attributed to changes in the metal surface state caused by hydrogen absorption.

Influence of hydrogen sorption on the surface composition of Pd alloys

Surface segregation is a common phenomenon in alloy systems. In this process, one of the constituents of the alloy preferentially diffuses to the surface, which results in a difference between the surface and bulk composition [398, 399]. When various strongly bounded adsorbates, such as hydrogen, are present on the surface, the process of surface segregation may be modified.

The influence of hydrogen electrosorption on surface segregation on Pd–Ag alloys was studied by Łukaszewski et al. [226] using the AES technique. The average surface content of Ag on freshly deposited Pd–Ag alloys was significantly higher than that in the bulk of the electrode, with the surface enrichment with Ag limited to the outermost atomic layers. On the other hand, the surface concentration of Pd on the hydrogen-treated sample was significantly higher than before hydrogen treatment; however, Pd surface concentration was still lower than that in the bulk of the alloy. This behavior was attributed to the reversed surface segregation of Pd–Ag alloy in the presence of electrosorbed hydrogen, predicted earlier theoretically [400].

Similar experiments were performed by Drążkiewicz et al. [232] for a Pd–Cu alloy. In contrast to the situation observed for Pd–Ag alloys, the surface composition of Pd–Cu alloys was close to their bulk composition and no influence of hydrogen electrosorption on the phase arrangement was detected.

Influence of surface oxidation on hydrogen electrosorption properties

Guerin and Attard [330] investigated the electrochemical behavior of nanostructured Pd–Pt alloys prepared by electrodeposition. They observed that during the electrode potential cycling in a full hydrogen–oxygen range, an additional pair of peaks appeared in the hydrogen region. These new signals did not arise when the electrode was polarized in the mere hydrogen region. The authors attributed the new peaks to hydrogen absorption/desorption into/from islands of pure Pd formed in the process of electrodissolution of Pd from the alloy and its subsequent redeposition proceeding together with the surface oxidation/oxide reduction during electrode polarization in the oxygen region.

A very similar effect was reported by Łukaszewski et al. [216] for Pd–Pt–Rh alloys subjected to potential cycling in the oxygen region. As the number of cycles increased, the new hydrogen peaks grew at the expense of the initial ones and finally became dominating signals in the hydrogen region. From the effect of sorption potential on the evolution of those signals and their strong electrochemical irreversibility, as well as on the basis of a negligible effect from reduced CO_2 [213], it was concluded that the new peaks originated mainly from bulk processes, i.e., hydrogen absorption and desorption. Since in the course of H/M vs. potential plots the region of the phase transition was split into two distinct regions, resembling hydrogen pressure–concentration isotherms for a system that has undergone a phase separation [401], it was suggested that after potential cycling of a Pd–Pt–Rh alloy, two phases were present, the absorption properties of which were different. The relation of two hydrogen peaks with the alloy bulk heterogeneity was verified by the examination of an electrode prepared by Pd deposition on previously deposited homogeneous Pd–Pt–Rh alloy [216].

Stresses induced by absorbed hydrogen

Hydrogen insertion into Pd and other metals results in changes in crystal lattice dimensions inducing stresses within the solid. Since these processes lead to the degradation of the absorbing material (hydrogen embrittlement), the phenomenon of stresses accompanying hydrogen

absorption was intensively studied using various techniques [53, 55, 129–157, 180].

Interestingly, the use of LVEs coincided with the rapid development of the quartz crystal microbalance method for electrochemical purposes [402–408]. Since the signal of the electrochemical quartz crystal microbalance is a function of a series of parameters, including the mass of absorbed gas and stresses in the metal, this technique was applied for studies on hydrogen absorption in Pd. It should be added that due to the very principles of the operation of the EQCM, in these experiments, the use of a thin layer of metal (usually below 0.5 μm) deposited on the surface of the quartz crystal is required. Thus, the LVE methodology is well fitted to the EQCM technique.

As demonstrated by Gräsjo and Seo [144], Bucur and Flanagan [145], as well as Cheek and O'Grady [141, 142], the EQCM response during hydrogen uptake markedly deviates from that predicted by the Sauerbrey equation describing the mass effects and can be attributed not only to the mass changes but also to the stresses generated inside the metal. These differences depend on the phase of absorbed hydrogen and the type of quartz crystals used. For AT-cut resonators, an additional negative frequency shift due to hydrogen absorption was observed, while for BT-cut resonators the stress-related effect was opposite. On the basis of complementary behavior of AT- and BT-cut quartz crystals the "double resonator method" was proposed [141, 142, 409, 410].

The EQCM response in the case of hydrogen electrosorption is determined mainly by two factors: (1) electrode mass changes (i.e., changes in the amount of electrosorbed hydrogen) and (2) stresses in the crystal lattice induced by hydrogen absorption. Therefore, the following equation is valid [55, 142, 148, 152–154]:

$$\Delta f = \Delta f_{\mathrm{mass}} + \Delta f_{\mathrm{stress}} \tag{6}$$

where Δf is the total measured frequency shift, Δf_{mass} is the contribution due to mass change, and $\Delta f_{\mathrm{stress}}$ is the contribution due to stresses. Since the mass of electrosorbed hydrogen is known from an electrochemical measurement (from the charge consumed in the process), it is possible to calculate—via the Sauerbrey equation [411]—the term Δf_{mass} and then to separate the term $\Delta f_{\mathrm{stress}}$ from the total measured frequency shift. $\Delta f_{\mathrm{stress}}$ can be a good parameter for a comparison of the stress effects between samples of known thicknesses.

According to EerNisse [409, 410], the values of $\Delta f_{\mathrm{stress}}$ can be recalculated into the average stress τ in a thin film of thickness, t_{f}, following the equation:

$$\tau = \left(\Delta f_{\mathrm{stress}} \cdot t_{\mathrm{q}}\right) / \left(k \cdot f_{\mathrm{q}} \cdot t_{\mathrm{f}}\right) \tag{7}$$

where t_{q} is the thickness of the quartz crystal (e.g., 166 μm for 10-MHz crystals), k is the stress coefficient (-2.75×10^{-11} $\mathrm{m^2N^{-1}}$ for AT-cut crystals), and f_{q} is the fundamental frequency of the quartz crystal.

Another parameter used in the literature for the EQCM data interpretation is the apparent molar mass of hydrogen, which is based upon the relation between the total measured frequency shift and charge due to hydrogen uptake, according to the equation [53, 55, 143, 146, 152, 153, 405]:

$$M_{\mathrm{a}} = -(\Delta f \cdot C \cdot F)/Q \tag{8}$$

where Δf is the total frequency shift, C is calibration constant of the quartz crystal resonator, F is Faraday's constant, and Q is the charge corresponding to the amount of electrosorbed hydrogen. The deviation of the apparent molar mass from the real molar mass of hydrogen (1 $\mathrm{gmol^{-1}}$) can be treated as a measure of the stress effects. The value of M_{a} shows how much the total observed frequency shift (resulting from both mass and stress) exceeds the pure mass effect.

Grdeń et al. [53, 143] used EQCM coupled with cyclic voltammetry and chronoamperometry to study hydrogen electrosorption in Pd in acidic and basic solutions. They confirmed earlier reports that the quartz crystal frequency is markedly affected by stresses generated inside the metal by absorbed hydrogen. The changes in frequency were nonlinear with respect to the changes in the amount of absorbed hydrogen, which excluded the possibility of the precise determination of the amount of absorbed hydrogen directly from the EQCM response. However, the EQCM appeared to be a promising tool for the studies on the stress effect itself. The apparent molar mass of absorbed hydrogen in the β-phase was in the range of 2–3 $\mathrm{gmol^{-1}}$ for both acidic and basic solutions. Similar values were reported by Gabrielli et al. [147]. On the other hand, the M_{a} values for the α-phase were approximately two times higher in base than in acid [143]. The differences were ascribed to the different effects of alkali metal incorporation and anion adsorption in both types of solutions [143].

Using EQCM, Grdeń et al. [146, 152] also studied hydrogen electrosorption in Pd–Ni alloys. Similar to the case of pure Pd, the values of the apparent molar mass of hydrogen exceeded 1 $\mathrm{gmol^{-1}}$, but for a given amount of absorbed hydrogen, they were also higher than those for pure Pd. It was explained taking into account that due to the crystal lattice contraction upon Pd alloying with Ni, the relative increase in the unit cell during hydrogen uptake was greater than for Pd, resulting in higher stresses. These results were in line with the opposite effect observed by Liu et al. [148] for Pd–Ag alloys where due to lattice expansion the stresses were weaker. On the basis of the EQCM data,

Grdeń et al. [146] suggested that the sharp decrease in the ability to absorb hydrogen for Pd–Ni alloys containing approx. 25–30% Ni was caused by crystal lattice contraction leading to a significant increase in stresses accompanying hydrogen insertion. Due to the latter effect, an additional portion of energy is required for hydrogen ingress into the alloy, making this process thermodynamically less favorable. It was also demonstrated that the quartz crystal response during hydrogen removal depends on the initial amount of absorbed hydrogen [152]. This effect was attributed to the differences in stress distributions in Pd–Ni alloys of various compositions and absorption of different amounts of hydrogen. It means that the stresses are not only the function of the current amount of dissolved hydrogen but also depend on the initial conditions of the desorption process.

Łukaszewski and Czerwiński [55, 153, 156, 157], as well as Żurowski et al. [154], continued the EQCM studies on hydrogen electrosorption in Pd alloys with Pt, Au, and Rh. The authors used Eq. 6 to extract the stress-related frequency shift from the total measured frequency shift. They found the resonator response to be dependent not only on alloy composition and the amount of absorbed hydrogen but also on the direction of the electrosorption process, i.e., absorption or desorption. The changes in the resonator frequency with the amount of hydrogen dissolved inside the metal were different during absorption and desorption, suggesting the different magnitude and distribution of stresses in each process. The differences in the frequency between the absorption and desorption courses for Pd alloys were smaller than for pure Pd, which correlated with the smaller extent of hysteresis for the alloys as compared with Pd. The results confirmed the important role of stress effect in the phenomenon of absorption/desorption hysteresis [55, 153].

Łukaszewski and Czerwiński [55, 153] used the EerNisse [409, 410] equation to calculate the average stress in thin films of Pd and Pd alloys with Pt, Au, and Rh from the stress-related frequency shift. The obtained values were in good agreement with those reported earlier [141, 148] and were close to the values calculated simply from the product of Young's modulus of the electrode materials [167, 168] and the relative increase in lattice parameter during hydrogen absorption [124, 125]. A correlation was found between stress magnitude and the relative change in crystal lattice dimensions during hydrogen uptake [153].

Other aspects of the electrochemical behavior of Pd-based LVEs (surface oxide formation/reduction, metal electrodissolution, adsorption of carbon oxides) were studied using EQCM by Grdeń et al. [412, 413], Łukaszewski et al. [54–56, 64, 67, 157, 218, 225], and Siwek et al. [66]

LVEs in applied electrochemistry

The unique features of LVEs have been utilized not only for fundamental studies but also in some areas of applied electrochemistry. Below, examples are shown of the applications of the LVE methodology in the context of electrochemical power sources, such as supercapacitors or hydride batteries.

Use of LVEs in electrochemical capacitors

Since hydrogen can be electrochemically inserted into and extracted from Pd-based electrodes, such materials can be treated as phase charging–discharging systems for electrochemical capacitors. These devices usually utilize the capacitance of electrical double layer of various carbon materials or pseudocapacitance connected with reversible redox processes like the insertion of atomic species into the crystal structure of bulk solid electrodes, e.g., conducting polymers or transition metal oxides (e.g., RuO_2, IrO_2, MnO_2) [414–419]. Due to the high currents generated during hydrogen uptake and removal as well as the good practical reversibility of these processes, thin Pd-based layers electrolytically loaded with hydrogen seem particularly promising for that purpose.

Czerwiński et al. [17, 18, 20] and Łukaszewski et al. [19] deposited thin layers of Pd and Pd–Rh alloys (92–97% Pd in the bulk) on reticulated vitreous carbon (RVC). RVC is an inexpensive and chemically inert carbon material characterized by an open-pore structure and highly developed surface [420–422]. Due to its unique properties, RVC is attractive for electrochemical studies as a substrate for the deposition of various metals studies and can be regarded as an electrode matrix applicable to energy storage systems [20, 422–431].

The amount of hydrogen absorbed in Pd-based deposits on RVC was recalculated into units commonly used for the description of energy storage systems, i.e., pseudocapacitance per unit of total mass of deposit and RVC substrate [432]. The maximum values of specific pseudocapacitance calculated per mass of the electroactive materials ranged from 3,100 to 4,900 $F g^{-1}$ [17–20]. The values recalculated per total mass of the deposit and RVC substrate reached 430 $F g^{-1}$ for Pd and 540 $F g^{-1}$ for Pd–Rh alloys [17–20], i.e., were comparable with the values reported for supercapacitors based on faradaic reactions and higher than those typical of double-layer capacitors [414–419]. The values of specific power were in the range 0.5–6.0 $W g^{-1}$, i.e., of the same order of magnitude as the characteristics of typical supercapacitors. Moreover, the maximum values of specific energy exceeded 20 Wh kg^{-1}, again within the range reported in the literature for this class of systems [414–419].

Use of LVEs in studies on electrode materials for hydride batteries

The methodology elaborated for fundamental studies on hydrogen electrosorption in Pd can be utilized for applied research, which was demonstrated in the examination of the electrochemical behavior of commercial AB_5-type alloys for hydride batteries. By extending the concept of LVEs to studies on MH-forming electrode materials, Piela et al. [433] and Rogulski et al. [434] presented a simple experimental procedure for the determination of the key performance parameters (hydrogen absorption capacity, hydrogen diffusion coefficient) characteristic of the particles of the MH-forming metal powder.

The MH alloy powder of an AB_5 type (LaMm-$Ni_{4.1}Al_{0.3}Mn_{0.4}Co_{0.45}$) with a fine Au metal wire mesh was pressed in a laboratory mechanical press into a thin (approx. 50-μm thickness) disk mounted in a gold net serving as an inert support and a current collector. The prepared electrode held a few milligrams of the active material and contained no inert binder material admixed to the active material. It was shown using cycling voltammetry and electrochemical impedance spectroscopy that the electrode exhibits features of single-particle electrodes, being suitable for a direct determination of the characteristic of the active particles without the need to resort to a complicated porous electrode modeling, which is required in the case of a procedure commonly applied in electrochemical studies on commercial MH alloys. Cyclic voltammetric curves recorded at sufficiently slow scan rates revealed well-defined hydrogen sorption and desorption peaks, well separated from the other faradaic processes. The MH LVE-type electrode was mechanically stable enough to allow a collection of a complete data set necessary for the kinetic and transport characterization of MH-forming particles [433, 434].

Thus, the benefits of LVE methodology have allowed studies on the intrinsic (i.e., without any influence of binder additives) electrochemical properties of the alloys destined for commercial Ni–MH batteries. Moreover, it has been suggested that by exploiting the thin layer concept, it may be possible to improve the performance of the electrochemical power sources based on hydrogen sorption process.

Concluding remarks

Undoubtedly, since the first use of a thin Pd layer for electrochemical studies on hydrogen absorption, our knowledge on this phenomenon has considerably grown. Investigations utilizing Pd LVEs provided invaluable information on the influence of electrode potential, temperature, electrolyte composition, electrode thickness, preparation conditions, and, in the case of Pd alloys, also of the addition of other metals on the process of hydrogen or deuterium electrosorption in these materials. Moreover, it became possible to study the interrelations between hydrogen absorption and other electrochemical phenomena taking place on Pd and its alloys, like the influence of hydrogen sorption on surface oxidation and phase segregation of Pd-based materials and, vice versa, the influence of surface processes like the adsorption of surface poisons on the bulk process of hydrogen insertion. The application of a thin metal layer in electrochemical experiments on hydrogen absorption in Pd has led to such interesting findings as the presence of the subsurface hydrogen, a direct path of hydrogen absorption or a dual mechanism of hydrogen desorption. These observations could not have been made when bulk electrodes had been used for that purpose. All these experiments, easy to perform on LVEs, would be very difficult or even impossible to carry out in the case of Pd electrodes made from wires or foils. Moreover, it was demonstrated that the LVE methodology could be utilized in applied electrochemistry, e.g., in electrochemical capacitors based on reversible hydrogen insertion/removal or in studies on new electrode materials for commercial nickel–hydride batteries. Thus, LVEs have created new possibilities for electrochemical studies on hydrogen-absorbing metals and alloys.

References

1. Hydrogen in metals I and II (1978) in: Alefeld G, Völkl J (eds) Topics in Applied Physics, vol. 28–29. Springer Verlag, Berlin, New York
2. Frumkin A (1963) In: Delahay P, Tobias CW (eds) Advances in electrochemistry and electrochemical engineering, vol. 3. New York, Interscience
3. Lewis FA (1967) The palladium-hydrogen system. Academic, London-New York
4. Pound BG (1993) In: Bockris JO'M (ed) Modern aspects of electrochemistry, no. 25. Plenum Press, New York
5. Oates WA, Flanagan TB (1981) Prog Solid St Chem 13:193–283
6. Oates WA, Flanagan TB (1991) Annu Rev Mater Sci 21:269–304
7. McLellan RB, Harkins CG (1975) Mater Sci Eng 18:5–35
8. Baranowski B, Filipek SM (2005) J Alloy Comp 404–406:2–6
9. Staliński B, Terpiłowski J (1987) Hydrogen and hydrides (in Polish). WNT, Warsaw
10. Amandusson H, Ekedahl L-G, Dannetun H (2001) J Membr Sci 193:35–47
11. Pizzi D, Worth R, Giacinti Baschetti M, Sarti GC, Noda K (2008) J Membr Sci 325:446–453
12. Crabtree GW, Dresselhaus MS, Buchanan MV (2004) Physics Today 57:39–44
13. Schlapbach L, Züttel A (2001) Nature 414:353–358
14. Kijeński J (2005) Przem Chem 84:799–807
15. Linden D, Reddy TB (2001) Handbook of batteries, 3rd edn. McGraw-Hill, New York

16. Kleperis J, Wójcik G, Czerwiński A, Skowroński J, Kopczyk M, Bełtowska-Brzezinska M (2001) J Solid State Electrochem 5:229–249
17. Czerwiński A, Łukaszewski M, Żurowski A, Patent RP 204948
18. Czerwiński A, Łukaszewski M, Żurowski A, Siwek H, Obrębowski S (2006) J New Mat Elect Syst 9:419–429
19. Łukaszewski M, Żurowski A, Czerwiński A (2008) J Power Sources 185:1598–1604
20. Czerwiński A, Rogulski Z, Obrębowski S, Siwek H, Paleska I, Chotkowski M, Łukaszewski M (2009) J Appl Electrochem 559–567
21. Sokolski DV (1962) Hydrogenation in solutions. Nauka, Alma-Ata
22. Geng M, Han J, Feng F, Northwood DO (1998) Int J Hydrog Energy 23:1055–1060
23. Czerwiński A, Rogulski Z, Dłubak J, Gumkowska A, Karwowska M (2009) Przem Chem 88:642–648
24. Feng F, Geng M, Northwood DO (2001) Int J Hydrog Energy 26:725–734
25. Hong K (2001) J Power Sources 96:85–89
26. Zhao X, Ma L (2009) Int J Hydrog Energy 34:4788–4796
27. Nakatsuka K, Yoshino M, Yukawa H, Morinaga M (1999) J Alloy Comp 293–295:222–226
28. Reilly JJ, Adzic GD, Johnson JR, Vogt T, Mukerjee S (1999) McBreen J 293–295:569–582
29. Di Profio P, Arca S, Rossi F, Filipponi M (2009) Int J Hydrog Energy 34:9173–9180
30. Vojtěch D, Šuštaršič B, Mortaniková M, Michalcová A, Veselá A (2009) Int J Hydrog Energy 34:7239–7245
31. Züttel A (2004) Naturwissenschaften 91:157–172
32. Jain IP, Jain P, Jain A (2010) J Alloy Comp 503:303–339
33. Sandrock (1999) J Alloy Comp 293–295:877–888
34. Güther V, Otoo A (1999) J Alloy Comp 293–295:889–892
35. Morinaga M, Yukawa H, Nakatsuka K, Takagi M (2002) J Alloy Comp 330–332:20–24
36. Grochala W, Edwards PP (2004) Chem Rev 104:1283–1315
37. Bououdina M, Grant D, Walker G (2006) Int J Hydrog Energy 31:177–182
38. Orimo S-I, Nakamori Y, Eliseo JR, Züttel A, Jensen CM (2007) Chem Rev 107:4111–4132
39. Sakintuna B, Lamari-Darkrim F, Hirscher M (2007) Int J Hydrog Energy 32:1121–1140
40. Cherry RS (2004) Int J Hydrog Energy 29:125–129
41. Hanneken JW (1999) Int J Hydrog Energy 24:1005–1026
42. Conway BE (1995) Prog Surf Sci 49:331
43. Burke LD (1980) Oxide growth and oxygen evolution on noble metals. In: Trasatti S (ed) Electrodes of conductive metallic oxides. Elsevier, New York, pp 141–181
44. Jerkiewicz G (1999) Surface oxidation of noble metal electrodes. In: Wieckowski A (ed) Interfacial electrochemistry. Marcel Dekker, New York, pp 559–576
45. Woods R (1976) Chemisorption at electrodes. In: Bard AJ (ed) Electroanalytical chemistry, vol. 9. Marcel Dekker, New York, pp 2–162
46. Dall'Antonia LH, Tremiliosi-Filho G, Jerkiewicz G (2001) J Electroanal Chem 502:72–81
47. Jerkiewicz G (1998) Prog Surf Sci 57:137–186
48. Rand DAJ, Woods R (1972) J Electroanal Chem 35:209–218
49. Schumacher R, Helbig W, Hass I, Wünsche M, Meyer H (1993) J Electroanal Chem 354:59–70
50. Bolzán AE, Martins ME, Arvía AJ (1984) J Electroanal Chem 172:221–233
51. Solomun T (1991) J Electroanal Chem 302:31–46
52. Cadle SH (1974) J Electrochem Soc 121:645–648
53. Grdeń M, Kotowski J, Czerwiński A (1999) J Solid State Electrochem 3:348–351
54. Łukaszewski M, Czerwiński A (2006) J Electroanal Chem 589:38–45
55. Łukaszewski M, Czerwiński A (2007) Pol J Chem 81:847–864
56. Łukaszewski M, Czerwiński A (2009) J Alloy Comp 473:220–226
57. Juodkazis K, Juodkazytė J, Šebeka B, Stalnionis G, Lukinskas A (2003) Russian J Electrochem 39:954–959
58. Gossner K, Mizera E (1979) J Electroanal Chem 98:37–48
59. Gossner K, Mizera E (1982) J Electroanal Chem 140:35–45
60. Nishimura K, Kunimatsu K, Enyo M (1989) J Electroanal Chem 260:167–179
61. Papageorgopoulos DC, Keijzer M, Veldhuis JBJ, de Bruijn FA (2002) J Electrochem Soc 149:A1400–A1404
62. Waszczuk P, Barnard TM, Rice C, Masel RI, Wieckowski A (2002) Electrochem Commun 4:599–603
63. Yépez O, Scharifker BR (1999) J Appl Electrochem 29:1185–1190
64. Łukaszewski M, Czerwiński A (2007) J Electroanal Chem 606:117–133
65. Łukaszewski M, Czerwiński A (2007) J Solid State Electrochem 11:339–349
66. Siwek H, Łukaszewski M, Czerwiński A (2008) Phys Chem Chem Phys 10:3752–3765
67. Łukaszewski M, Siwek H, Czerwiński A (2010) J Solid State Electrochem 14:1279–1292
68. Garcia AC, Paganin VA, Ticianelli EA (2008) Electrochim Acta 53:4309–4315
69. Schmidt TJ, Jusys Z, Gasteiger HA, Behm RJ, Endruschat U, Boennemann H (2001) J Electroanal Chem 501:132–140
70. He C, Kunz HR, Fenton JM (1997) J Electrochem Soc 144:970–979
71. Yépez O, Pickup PG (2005) Electrochem Solid-State Lett 8: E35–E38
72. Soszko M, Łukaszewski M, Mianowska Z, Czerwiński A (2011) J Power Sorces 196:3513–3522
73. Fischer JM, Cabello-Moreno, Christian E, Thompsett D (2009) Electrochem Solid State Lett 12:B77–B81
74. Bianchini C, Shen PK (2009) Chem Rev 109:4183–4206
75. Zhu LD, Zhao TS, Xu JB, Liang ZX (2009) J Power Sources 187:80–84
76. Xu JB, Zhao TS, Li YS, Yang WW (2010) Int J Hydrog Energy 35:9693–9700
77. Nguyen ST, Law HM, Nguyen HT, Kristian N, Wang S, Chan SH, Wang X (2009) Appl Catal B-En 91:507–515
78. Xu JB, Zhao TS, Shen SY, Li YS (2010) Int J Hydrog Energy 35:6490–6500
79. Cheng F, Dai X, Wang H, Jiang SP, Zhang M, Xu C (2010) Electrochim Acta 55:2295–2298
80. Ding K, Yang G, Wei S, Mavinakuli P, Guo Z (2010) Ind Eng Chem Res 49:11415–11420
81. Machida K, Enyo M (1987) J Electrochem Soc 134:1472–1474
82. Beden B, Lamy C, Leger J-M (1979) Electrochim Acta 24:1157–1166
83. Nishimura K, Machida K, Enyo M (1988) J Electroanal Chem 251:103–116
84. Nishimura K, Machida K, Enyo M (1988) J Electroanal Chem 251:117–125
85. Nishimura K, Kunimatsu K, Machida K, Enyo M (1989) J Electroanal Chem 260:181–192
86. Enyo M (1985) J Electroanal Chem 186:155–166
87. Hoshi N, Kida K, Nakamura M, Nakada M, Osada K (2006) J Phys Chem B 110:12480–12484
88. Rice C, Ha S, Masel RI, Wieckowski A (2003) J Power Sources 115:229–235
89. Zhou WP, Lewera A, Larsen R, Masel RI, Bagus PS, Wieckowski A (2006) J Phys Chem B 110:13393–13398

90. Chen C-H, Liou W-J, Lin H-M, Wu S-H, Mikołajczuk A, Stobiński L, Borodziński A, Kędzierzawski P, Kurzydłowski K (2010) Phys Status Solidi A 207:1160–1165
91. Chen CH, Liou WJ, Lin HM, Wu SH, Borodziński A, Stobiński L, Kędzierzawski P (2010) Fuel Cells 10:227–233
92. Baldauf M, Kolb DM (1996) J Phys Chem 100:11375–11381
93. Jiang J, Kucernak A (2009) Electrochim Acta 54:4545–4551
94. Liu B, Li HY, Die L, Zhang XH, Fan Z, Chen JH (2009) J Power Sources 186:62–66
95. Winjobi O, Zhang Z, Liang C, Li* W (2010) Electrochim Acta 55:4217–4221
96. Miyake H, Okada T, Samjeské G, Osawa M (2008) Phys Chem Chem Phys 10:3662–3669
97. Yi Q, Huang W, Liu X, Xu G, Zhou Z, Chen A (2008) J Electroanal Chem 619–620:197–205
98. Yépez O, Scharifker BR (2002) Int J Hydrog Energy 27:99–105
99. Damjanovic A, Brusić V (1967) J Electroanal Chem 15:29–33
100. Damjanovic A, Brusić V (1967) Electrochmi Acta 12:1171–1184
101. Jung D, Beak S, Nahm KS, Kim P (2010) Korean J Chem Eng 27:1689–1694
102. Fouda-Onana F, Bah S, Savadogo O (2009) J Electroanal Chem 636:1–9
103. Erikson H, Kasikov A, Johans C, Kontturi K, Tammeveski K, Sarapuu A (2011) J Electroanal Chem 652:1–7
104. Lopes T, Antolini E, Gonzalez ER (2008) Int J Hydrog Energy 33:5563–5570
105. Salvador-Pascual JJ, Citalán-Cigarroa S, Solorza-Feria O (2007) J Power Sources 172:229–234
106. Guerin S, Hayden BE, Lee CE, Mormiche C, Russell AE (2006) J Phys Chem B 110:14355–14362
107. Nilekar AU, Xu Y, Zhang J, Vukmirovic MB, Sasaki K, Adzic RR, Mavrikakis M (2007) Top Catal 46:276–284
108. Sarapuu A, Kasikov A, Wong N, Lucas CA, Sedghi G, Nichols RJ, Tammeveski K (2010) Electrochim Acta 55:6768–6774
109. Wang W, Huang Q, Liu J, Zou Z, Li Z, Yang H (2008) Electrochem Commun 10:1396–1399
110. Shao MH, Huang T, Liu P, Zhang J, Sasaki K, Vukmirovic MB, Adzic RR (2006) Langmuir 22:10409–10415
111. Savadogo O, Lee K, Oishi K, Mitsushima S, Kamiya N, Ota K-I (2004) Electrochem Commun 6:105–109
112. Pluntke Y, Kibler LA, Kolb DM (2008) Phys Chem Chem Phys 10:3684–3688
113. Francisco Alcaide, Álvarez G, Cabot PL, Miguel O, Querejeta A (2010) Int J Hydrog Energy 35:11634–11641
114. Schuldiner S, Hoare JP (1957) J Phys Chem 61:705–708
115. Grdeń M, Łukaszewski M, Jerkiewicz G, Czerwiński A (2008) Electrochim Acta 53:7583–7598
116. Flanagan TB, Lewis FA (1959) Trans Faraday Soc 55:1400–1408
117. Flanagan TB, Lewis FA (1959) Trans Faraday Soc 55:1409–1420
118. Flanagan TB (1961) J Phys Chem 65:280–284
119. Lewis FA (1960) Plat Met Rev 4:132–137
120. Lewis FA (1961) Plat Met Rev 5:21–25
121. Lewis FA (1982) Plat Met Rev 26:20–27
122. Lewis FA (1982) Plat Met Rev 26:70–78
123. Lewis FA (1982) Plat Met Rev 26:121–128
124. Sakamoto Y, Baba K, Flanagan TB (1988) Z Phys Chem NF 158:223–235
125. Sakamoto Y, Yuwasa K, Hirayama K (1982) J Less-Common Met 88:115–124
126. Czerwiński A, Marassi R, Zamponi S (1991) J Electroanal Chem 316:211–220
127. Czerwiński A, Marassi R (1992) J Electroanal Chem 322:373–381
128. Czerwiński A (1995) Pol J Chem 69:699–706
129. Wriedt HA, Oriani RA (1970) Acta Metal 18:753–760
130. Heusler KE, Pietrucha J (1992) J Electroanal Chem 329:339–350
131. Kandasamy K (1995) Int J Hydrog Energy 20:455–463
132. Fenzl W, Zabel H, Peisl H (1982) J Phys F Met Phys 12:1897–1906
133. Han J-N, Lee J-W, Seo M, Pyun S-I (2001) J Electroanal Chem 506:1–10
134. Han J-N, Pyun S-I, Kim D-J (1999) Electrochim Acta 44:1797–1804
135. Pedersen TPL, Liesch C, Salinga C, Eleftheriadis T, Weis H, Wuttig M (2004) Thin Solid Films 458:299–303
136. De Ninno A, Violante V, La Barbera A (1997) Phys Rev B 56:2417–2420
137. Hu Z, Thundat T, Warmack RJ (2001) J Appl Phys 90:427–431
138. Stafford GR, Bertocci U (2009) J Phys Chem C 113:13249–13256
139. Pivak Y, Schreuders H, Slaman M, Griessen R, Dam B (2011) Int J Hydrog Energy 36:4056–4067
140. Zoltowski P (1999) Electrochim Acta 44:4415–4429
141. Cheek GT, O'Grady WE (1990) J Electroanal Chem 277:341–346
142. Cheek GT, O'Grady WE (1994) J Electroanal Chem 368:133–138
143. Grdeń M, Kotowski J, Czerwiński A (1999) J Solid State Electrochem 4:273–278
144. Gräsjo L, Seo M (1990) J Electroanal Chem 296:233–239
145. Bucur RV, Flanagan TB (1974) Z Phys Chem NF 88:225–241
146. Grdeń M, Kuśmierczyk K, Czerwiński A (2002) J Solid State Electrochem 7:43–48
147. Gabrielli C, Grand PP, Lasia A, Perrot H (2002) Electrochim Acta 2199–2207
148. Liu S-Y, Kao Y-H, Su YO, Perng T-P (1999) J Alloy Comp 293–295:468–471
149. Liu S-Y, Kao Y-H, Su YO, Perng T-P (2000) J Alloy Comp 311:283–287
150. Liu S-Y, Kao Y-H, Su YO, Perng T-P (2001) J Alloy Comp 316:280–283
151. Yamamoto N, Ohsaka T, Terashima T, Oyama N (1990) J Electroanal Chem 296:463–471
152. Grdeń M, Klimek K, Czerwiński A (2006) Electrochim Acta 51:2221–2229
153. Łukaszewski M, Czerwiński A (2006) J Electroanal Chem 589:87–95
154. Żurowski A, Łukaszewski M, Czerwiński A (2006) Electrochim Acta 51:3112–3117
155. Łukaszewski M, Kędra T, Czerwiński A (2010) Electrochim Acta 55:1150–1159
156. Łukaszewski M, Czerwiński A (2008) J Solid State Electrochem 12:1589–1598
157. Łukaszewski M, Czerwiński A (2007) Przem Chem 86:846–853
158. Kandasamy K, Lewis FA, Sakamoto Y, Tong XQ (1999) Int J Hydrog Energy 24:759–761
159. Fazle Kibria AKM, Kubota T, Kagawa A, Sakamoto Y (1999) Int J Hydrog Energy 24:747–757
160. Fazle Kibria AKM, Sakamoto Y (1997) Mat Sci Eng B 49:227–232
161. Lewis FA, Kandasamy K, McNicholl R-A, Tong XQ (1995) Int J Hydrog Energy 20:369–372
162. Fazle Kibria AKM, Sakamoto Y (1998) Int J Hydrog Energy 23:475–481
163. Xu ZR, Maroevic P, McLellan RB (1998) J Alloy Comp 279:259–262
164. Zhang W-S, Zhang Z-F, Zhang Z-L (2002) J Electroanal Chem 528:1–17
165. Tripodi P, Di Gioacchino D, Vinko JD (2009) J Alloy Comp 486:55–59
166. Lee E, Lee JM, Koo JH, Lee W, Lee T (2010) Int J Hydrog Energy 35:6984–6991

167. Fabre A, Finot E, Demoment J, Contreras S (2003) Ultramicroscopy 97:425–432
168. Fabre A, Finot E, Demoment J, Contreras S (2003) J Alloy Comp 356–357:372–376
169. Dahlmeyer J, Garrison T, Garrison T, Darkey S, Massicotte F, Rebeiz K, Nesbit S, Craft A (2011) Scripta Mater 64:789–792
170. Dillon E, Jimenez G, Davie A, Bulak J, Nesbit S, Craft A (2009) Mater Sci Eng A 524:89–97
171. Jerkiewicz G, Zolfaghari A (1996) J Electrochmem Soc 143:1240–1248
172. Rand DAJ, Woods R (1975) Anal Chem 47:1481–1483
173. Woods R (1969) Electrochim Acta 14:632–635
174. Rand DAJ, Woods R (1973) J Electroanal Chem 44:83–89
175. Cadle SH (1974) Anal Chem 46:587–590
176. Bucur RV, Stoicovici L (1970) J Electroanal Chem 25:342–343
177. Bucur RV, Mecea V, Indrea E (1976) J Less-Common Met 49:147–158
178. Chevillot J-P, Farcy J, Hinnen C, Rousseau A (1975) J Electroanal Chem 64:39–62
179. Frazier GA, Glosser R (1980) J Less-Common Met 74:89–96
180. Bucur RV, Mecea V (1980) Surf Techn 11:305–322
181. Horkans J (1980) J Electroanal Chem 106:245–249
182. Nicolas M, Dumoulin L, Burger JP (1986) J Appl Phys 60:3125–3130
183. Nicolas M, Raffy H, Dumoulin L, Burger JP (1987) J Less-Common Met 130:61–67
184. Gossner K, Mizera E (1981) J Electroanal Chem 125:359–366
185. Harris (1982) J Electrochem Soc 129:2689–2694
186. Rosamilia JM, Abys JA, Miller B (1991) Electrochim Acta 36:1203–1208
187. Tateishi N, Yahikozawa K, Nishimura K, Suzuki M, Iwanaga Y, Watanabe M, Enami E, Matsuda Y, Takasu Y (1991) Electrochim Acta 36:1235–1240
188. Tateishi N, Yahikozawa K, Nishimura K, Takasu Y (1992) Electrochim Acta 37:2427–2432
189. Attard GA, Bannister A (1991) J Electroanal Chem 300:467–485
190. Attard GA, Price R, Al-Akl A (1994) Electrochim Acta 39:1525–1530
191. Szpak S, Mosier-Boss PA, Scharber SR, Smith JJ (1992) J Electroanal Chem 337:147–163
192. Czerwiński A, Zamponi S, Marassi R (1991) J Electroanal Chem 304:233–239
193. Czerwiński A, Maruszczak G, Żelazowska M (1993) Pol J Chem 67:2037–2046
194. Czerwiński A (1994) Electrochim Acta 39:431–436
195. Czerwiński A (1994) J Electroanal Chem 379:487–494
196. Czauderna M, Maruszczak G, Czerwiński A (1995) J Radioanal Nucl Chem Lett 199:375–383
197. Czerwiński A, Maruszczak G, Żelazowska M, Łańcucka M, Marassi R, Zamponi S (1995) J Electroanal Chem 386:207–211
198. Maruszczak G, Czerwiński A (1995) Anal Lett 28:547–2560
199. Czerwiński A, Frydrych J, Kiersztyn I (1996) Anal Lett 29:2549–2561
200. Czerwiński A, Czauderna M, Maruszczak G, Kiersztyn I, Marassi R, Zamponi S (1997) Electrochim Acta 42:81–86
201. Grdeń M, Czerwiński A, Golimowski J, Bulska E, Krasnodębska-Ostręga B, Marassi R, Zamponi S (1999) J Electroanal Chem 460:30–37
202. Czerwiński A, Kiersztyn I, Grdeń M, Czapla J (1999) J Electroanal Chem 471:190–1951
203. Czerwiński A, Kiersztyn I, Grdeń M (2000) J Electroanal Chem 492:128–136
204. Rusanova MY, Grdeń M, Czerwiński A, Tsirlina GA, Petrii OA, Safonowa TY (2001) J Solid State Electrochem 5:212–220
205. Grdeń M, Paruszewska A, Czerwiński A (2001) J Electroanal Chem 502:91–99
206. Grdeń M, Piaścik A, Koczorowski Z, Czerwiński A (2002) J Electroanal Chem 532:35–42
207. Łukaszewski M, Kuśmierczyk K, Kotowski J, Siwek H, Czerwiński A (2003) J Solid State Electrochem 7:69–76
208. Czerwiński A, Kiersztyn I, Grdeń M (2003) J Solid State Electrochem 7:321–326
209. Łukaszewski M, Czerwiński A (2003) Electrochim Acta 48:2435–2445
210. Łukaszewski M, Grdeń M, Czerwiński A (2004) J Phys Chem Solids 65:523–530
211. Łukaszewski M, Grdeń M, Czerwiński A (2004) Anal Lett 37:967–978
212. Czerwiński A, Grdeń M, Łukaszewski M (2004) J Solid State Electrochem 8:411–415
213. Łukaszewski M, Grdeń M, Czerwiński A (2004) Electrochim Acta 49:3161–3316
214. Siwek H, Łukaszewski M, Czerwiński A (2004) Pol J Chem 78:1121–1134
215. Czerwiński A, Łukaszewski M, Grdeń M, Siwek H (2004) Przem Chem 83:180–185
216. Łukaszewski M, Grdeń M, Czerwiński A (2004) J Electroanal Chem 573:87–98
217. Łukaszewski M, Grdeń M, Czerwiński A (2005) J Solid State Electrochem 9:1–10
218. Łukaszewski M, Czerwiński A (2006) Electrochim Acta 51:4728–4735
219. Czerwiński A (2006) Przem Chem 85:1186–1189
220. Łukaszewski M, Grdeń M, Czerwiński A (2006) J New Mater Elect Syst 9:409–417
221. Łukaszewski M, Grdeń M, Czerwiński A (2007) Przem Chem 86:137–142
222. Łukaszewski M, Żurowski A, Grdeń M, Czerwiński A (2007) Electrochem Commun 9:671–676
223. Łukaszewski M, Czerwiński A (2007) Przem Chem 86:1231–1236
224. Żurowski A, Łukaszewski M, Czerwiński A (2008) Electrochim Acta 53:7812–7816
225. Łukaszewski M, Kędra T, Czerwiński A (2009) Electrochem Commun 11:409–503
226. Łukaszewski M, Klimek K, Czerwiński A (2009) J Electroanal Chem 637:13–20
227. Łukaszewski M, Kędra T, Czerwiński A (2010) J Electroanal Chem 638:123–130
228. Łukaszewski M, Siwek H, Czerwiński A (2009) J Solid State Electrochem 13:813–827
229. Łukaszewski M, Czerwiński A (2010) Thin Solid Films 518:3680–3689
230. Łukaszewski M, Żurowski A, Kędra T, Czerwiński A (2010) Przem Chem 89:704–708
231. Łukaszewski M, Hubkowska K, Czerwiński A (2010) Phys Chem Chem Phys 12:14567–14572
232. Drążkiewicz K, Łukaszewski M, Czerwiński A (2010) Przem Chem 89:1053–1058
233. Hubkowska K, Łukaszewski M, Czerwiński A (2010) Electrochim Acta 56:235–242
234. Hubkowska K, Łukaszewski M, Czerwiński A (2011) Electrochim Acta 56:2344–2350
235. Łukaszewski M, Hubkowska K, Czerwiński A (2011) J Electroanal Chem 651:131–142
236. Soszko M, Łukaszewski M, Mianowska Z, Drążkiewicz K, Siwek K, Czerwiński A (2011) Przem Chem 90:1195–1200
237. Łukaszewski M, Klimek K, Żurowski A, Kędra T, Czerwiński A (2011) Solid State Ionics 190:18–24
238. Łukaszewski M, Hubkowska K, Czerwiński A (2011) Przem Chem 90:1201–1206

239. Koss U, Łukaszewski M, Hubkowska K, Czerwiński A (2011) J Solid State Electrochem, available on-line, doi:10.1007/s10008-011-1511-8
240. Czerwiński A, Kiersztyn I, Łukaszewski M, Grdeń M (2005) In: Birss V, Wieckowski A (eds), Electrocatalysis, pp 53–62, Electrochemical Society
241. Baldauf M, Kolb DM (1993) Electrochim Acta 38:2145–2153
242. Wen T-C, Hu C-C (1993) J Electrochem Soc 140:988–995
243. Hu C-C, Wen T-C (1994) J Electrochem Soc 141:2996–3001
244. Hu C-C, Wen T-C (1995) J Electrochem Soc 142:1376–1383
245. Podlovchenko BI, Kolyadko EA, Lu S (1995) J Electroanal Chem 399:21–27
246. Manolatos P, Jerome M (1996) Electrochim Acta 41:359–365
247. Li Y, Cheng Y-T (1996) Int J Hydrogen Energy 21:281–291
248. Giacomini MT, Balasubramanian, Khalid S, McBreen J, Ticianelli EA (2003) J Electrochem Soc 150:A588–A593
249. Winkler K, de Bettencourt-Dias A, Balch AL (2000) Chem Mater 12:1386–1392
250. Safonova TY, Khairullin DR, Tsirlina GA, Petrii OA, Vassiliev SY (2005) Electrochim Acta 50:4752–4762
251. Rusanova MY, Tsirlina GA, Petrii OA, Safonova TY, Vassiliev SY (2000) Russ J Electrochem 36:457–464
252. Roginskaya YE, Lubnin EN, Safonova TY, Chuvillin AL, Politova ED, Tsirlina GA (2003) Russ J Electrochem 39:253–262
253. Plyasova LM, Molina IY, Cherepanova SV, Rudina NA, Sherstyuk OV, Savinova ER, Pron'kin SN, Tsirlina GA (2002) Russ J Electrochem 38:1116–1131
254. Tsirlina GA, Nagaev EL, Rusanova (2000) Phys Lett A 267:71–80
255. Tsirlina GA, Baronov SB, Spiridonov FM, Rusanova MY, Safonova TY, Petrii OA (2000) Russ J Electrochem 36:1179–1185
256. Tsirlina GA, Petrii OA, Safonova TY, Papisov IM, Vassiliev SY, Gabrielov AE (2002) Electrochim Acta 47:3749–3758
257. Petrii OA, Safonova TY, Tsirlina GA, Rusanova MY (2000) Electrochim Acta 45:4117–4126
258. Bartlett PN, Gollas B, Guerin S, Marwan J (2002) Phys Chem Phys Chem 4:3835–3842
259. Bartlett PN, Marwan J (2004) Phys Chem Chem Phys 6:2895–2898
260. Rose A, Maniguet S, Mathew RJ, Slater C, Yao J, Russell AE (2003) Phys Chem Chem Phys 5:3220–3225
261. Paillier J, Roué L (2005) J Electrochem Soc 152:E1–E8
262. Gabrielli C, Grand PP, Lasia A, Perrot H (2004) J Electrochem Soc 151:A1925–A1936
263. Gabrielli C, Grand PP, Lasia A, Perrot H (2004) J Electrochem Soc 151:A1937–A1942
264. Gabrielli C, Grand PP, Lasia A, Perrot H (2004) J Electrochem Soc 151:A1943–A1949
265. Gabrielli C, Grand PP, Lasia A, Perrot H (2002) J Electroanal Chem 532:121–131
266. Łosiewicz B, Birry L, Lasia A (2007) J Electroanal Chem 611:26–34
267. Lasia A (2006) J Electroanal Chem 6593:159–166
268. Birry L, Lasia A (2006) Electrochim Acta 51:3356–3364
269. Martin MH, Lasia A (2009) Electrochim Acta 54:5292–5299
270. Martin MH, Lasia A (2008) Electrochim Acta 53:6317–6322
271. Duncan H, Lasia A (2007) Electrochim Acta 52:6195–6205
272. Duncan H, Lasia A (2008) Electrochim Acta 53:6845–6850
273. Duncan H, Lasia A (2008) J Electroanal Chem 621:62–68
274. Denuault G, Milhano C, Pletcher D (2005) Phys Chem Chem Phys 7:3545–3551
275. Frydrychewicz A, Bieguński AT, Jackowska K, Tsirlina GA (2008) J Solid State Electrochem 12:1085–1091
276. Frydrychewicz A, Vassiliev SY, Tsirlina GA, Jackowska K (2005) Electrochim Acta 50:1885–1893
277. Frydrychewicz A, Czerwiński A, Jackowska K (2001) Synth Met 121:1401–1402
278. Chu S-Z, Kawamura H, Mori M (2007) Electrochim Acta 92–99
279. Bouhtiyya S, Roué L (2008) Int J Hydrogen Energy 33:2912–2920
280. Lebouin C, Olivier YS, Sibert E, Millet P, Maret M, Faure R (2009) J Electroanal Chem 626:59–65
281. Oliveira MC (2006) Electrochem Commun 8:647–652
282. Oliveira MC (2006) Mater Sci Forum 514–516:456–459
283. Corduneanu O, Disculescu VC, Chiorcea-Paquin A-M, Oliveira-Brett A-M (2008) J Electroanal Chem 624:97–108
284. Bertoncello P, Peruffo M, Unwin PR (2007) Chem Commun 1597–1599
285. Scholl H, Błaszczyk T, Leniart A, Polański K (2004) J Solid State Electrochem 8:308–315
286. Skowroński JM, Czerwiński A, Rozmanowski T, Rogulski Z, Krawczyk P (2007) Electrochim Acta 52:5677–5684
287. Skowroński JM, Rozmanowski T, Krawczyk P, Rogulski Z, Czerwiński A (2008) J Nanosci Nanotechnol 8:1–8
288. Zhang W-S, Zhang X-W, Zhao X-G (1998) J Electroanal Chem 107–112
289. Skitał PM, Sanecki PT, Kaczmarski K (2010) Electrochim Acta 55:5604–5609
290. Galus Z (1994) Fundamentals of electrochemical analysis. Ellis Horwood, New York
291. Bard AJ, Faulkner LR (2001) Electrochemical methods. Fundamentals and applications, John Wiley & Sons, New York
292. Rand DAJ, Woods R (1972) J Electroanal Chem 36:57–69
293. Lee J-W, Pyun S-I (2005) Electrochim Acta 50:1777–1805
294. Zoltowski P (2007) J Electroanal Chem 600:54–62
295. Zakroczymski T (1999) J Electroanal Chem 475:82–88
296. Zakroczymski T (2006) Electrochim Acta 51:2261–2266
297. Millet P, Srour M, Faure R, Diamond R (2001) Electrochem Commun 3:478–482
298. Vasile MJ, Enke CG (1965) J Electrochem Soc 112:865–870
299. Wolfe RC, Weil KG, Shaw BA, Pickering HW (2005) J Electrochem Soc 152:B82–B88
300. Zoltowski P (2010) Electrochim Acta 55:6274–6282
301. Dębowska L, Baranowski B (2008) Pol J Chem 82:643–646
302. Vigier F, Jurczakowski R, Lasia A (2007) J Electroanal Chem 602:145–148
303. Enyo M (1973) Electrochim Acta 18:155–162
304. Enyo M (1973) Electrochim Acta 18:163–166
305. Enyo M (1994) Electrochim Acta 39:1715–1721
306. Maoka T, Enyo M (1981) Electrochim Acta 26:607–614
307. Maoka T, Enyo M (1981) Electrochim Acta 26:615–619
308. Vigier F, Jurczakowski R, Lasia A (2006) J Electroanal Chem 588:32–43
309. Lawson DR, Tierney MJ, Cheng IF, VanDyke LS, Espenscheid MW, Martin CR (1991) Electrochim Acta 36:1515–1522
310. Wang D, Flanagan TB, Kuji T (2002) Phys Chem Chem Phys 4:4244–4254
311. Flanagan TB, Clewley JD (1982) J Less-Common Met 83:127–141
312. Balasubramanian R (1997) J Alloy Comp 253–254:203–206
313. Balasubramanian R (1996) Int J Hydrogen Energy 21:119–127
314. Bowerman BS, Biehl GE, Wulff CA, Flanagan TB (1908) Ber Bunsenges Phys Chem 84:536–542
315. Flanagan TB, Park C-N, Oates WA (1995) Prog Solid St Chem 23:291–363
316. Baranowski B (1992) Wiad Chem 46:21–32 (in Polish)
317. Züttel A, Nützenadel C, Schmid G, Chartouni D, Schlapbach L (1999) J Alloy Comp 293–295:472–475
318. Züttel A, Nützenadel C, Schmid G, Emmenegger C, Sudan P, Schlapbach L (2000) Appl Surf Sci 162–163:571–575
319. Kuji T, Uchida H, Sato M, Cui W (1999) J Alloy Comp 293–295:19–22

320. Kishore S, Nelson JA, Adair JH, Eklund PC (2005) J Alloy Comp 389:234–242
321. Natter H, Wettmann B, Heisel B, Hempelmann R (1997) J Alloy Comp 253–254:84–86
322. Ruda M, Crespo EA, de Debiaggi SR (2010) 495:471–475
323. Lee MW, Wolf RJ, Ray JR (1995) J Alloy Comp 231:343–346
324. Kuji T, Matsumura Y, Uchida H, Aizawa T (2002) J Alloy Comp 330–332:718–722
325. Pundt A, Sachs C, Winter M, Reetz MT, Frish D, Kirchheim (1999) J Alloy Comp 293–295:480–483
326. Pundt A, Suleiman M, Bähtz C, Reetz MT, Kirchheim, Jisrawi NM (1999) Mater Sci Eng B 108:19–23
327. Suleiman M, Jisrawi NM, Dankert O, Reetz MT, Bähtz C, Kirchheim R, Pundt A (2003) J Alloy Comp 356–357:644–648
328. Suleiman M, Faupel J, Borchers C, Krebs H-U, Kirchheim R, Pundt A (2005) J Alloy Comp 404–406:523–528
329. Zhang W-S, Zhang Z-L, Zhang X-W (2000) J Electroanal Chem 481:13–23
330. Guerin S, Attard GS (2001) Electrochem Commun 3:544–548
331. Solla-Gullón J, Montiel V, Aldaz A, Clavilier J (2002) Electrochem Commun 4:716–721
332. Solla-Gullón J, Rodes A, Montiel V, Aldaz A, Clavilier J (2003) J Electroanal Chem 554–555:273–284
333. Solla-Gullón J, Montiel V, Aldaz A, Clavilier J (2003) J Electrochem Soc 150:E104–E109
334. Zoltowski P, Makowska E (2001) Phys Chem Chem Phys 3:2935–2942
335. Chen S, Adams BD, Chen A (2010) Electrochim Acta 56:61–67
336. Lasia A, Jurczakowski R, Łosiewicz B (2007) ECS Trans 2:11–19
337. Adams BD, Wu G, Nigro S, Chen A (2009) J Am Chem Soc 131:6930–6931
338. Adams BD, Ostrom CK, Chen A (2010) Langmiur 26:7632–7637
339. Słojewski M, Kowalska J, Jurczakowski R (2009) J Phys Chem C 113:3707–3712
340. Correia AN, Mascaro LH, Machado SAS, Avaca LA (1997) Electrochim Acta 42:493–495
341. Lee J-W, Pyun SI, Filipek S (2003) Electrochim Acta 48:1603–1611
342. Flanagan TB, Sakamoto Y (1993) Plat Met Rev 37:26–37
343. Sakamoto Y, Chen FI, Ura M, Flanagan TB (1995) Ber Bunsenges Phys Chem 99:807–820
344. Wicke E, Frölich K (1989) Z Phys Chem NF 163:35–40
345. Kandasamy K, Lewis FA, McFall WD, McNicholl R-A (1989) Z Phys Chem NF 163:41–46
346. Burch R (1970) Trans Faraday Soc 66:736–748
347. Maeland A, Flanagan TB (1965) J Phys Chem 69:3575–3581
348. Maeland A, Flanagan TB (1964) J Phys Chem 68:1419–1426
349. Moysan I, Paul-Boncour V, Thiébaut S, Sciora E, Fournier JM, Cortes R, Bourgeois S, Percheron-Guégan A (2001) J Alloys Comp 332:14–20
350. Thiébaut S, Bigot A, Achard JC, Limacher B, Leroy D, Percheron-Guégan A (1995) J Alloys Comp 231:440–447
351. Noh H, Flanagan TB, Sonoda T, Sakamoto Y (1995) J Alloys Comp 228:164–171
352. Sakamoto Y, Haraguchi Y, Ura M, Chen FL (1994) Ber Bunsenges Phys Chem 98:964–969
353. Lasia A, Grégoire D (1995) J Electrochem Soc 142:3393–3399
354. Perng TP, Wu JK (2003) Mater Lett 57:3437–3438
355. Valøen LO, Lasia A, Jensen JO, Tunold R (2002) Electrochimica Acta 47:2871–2884
356. Szpak S, Mosier-Boss PA, Gabriel CJ, Smith JJ (1994) J Electroanal Chem 365:275–281
357. Breiter MW (1978) Z Phys Chem NF 112:183–193
358. Bucur RV (1977) Surf Sci 62:519–535
359. Bucur RV, Covaci I (1979) Electrochim Acta 24:1213–1218
360. Bucur RV, Bota F (1982) Electrochim Acta 27:521–528
361. Conway BE, Wojtowicz J (1992) J Electroanal Chem 326:277–297
362. Conway BE (1993) Jerkiewicz G 357:47–66
363. Conway BE, Bai L (1986) J Electroanal Chem 198:149–175
364. Okuyama H, Siga W, Takagi N, Nishijima M, Aruga T (1998) Surf Sci 401:344–354
365. Bagotskaya (1962) Zhurn Phiz Khimii 36:2667–2673 (in Russian)
366. Breiter MW (1979) J Electroanal Chem 109:253–260
367. Artemenko YA, Goltsova MV, Zaitsev VI (1997) Int J Hydrogen Energy 22:343–345
368. Goltsova MV, Artemenko YA, Zaitsev VI (1999) J Alloy Comp 293–295:379–384
369. Skorodumov BG, Serebryakov VN, Ulanov VG, Zhukovska EV, Zhukovsky OA (1996) Int J Hydrogen Energy 21:961–968
370. Choi Y-M, Pyun S-I, Paulsen JM (1998) Electrochim Acta 44:623–632
371. Bennett PA, Fuggle JC (1982) Phys Rev B 26:6030–6039
372. Schuldiner S, Castellan GW, Hoare JP (1958) J Chem Phys 28:16–19
373. Yoshitake H, Muto G, Ota K (1996) J Electroanal Chem 401:81–87
374. Yamazaki O, Yoshitake H, Kamiya N, Ota K (1995) J Electroanal Chem 390:127–133
375. Enyo M, Biswas PC (1992) J Electroanal Chem 335:309–319
376. Yoshitake H, Yamazaki O, Ota K (1995) J Electroanal Chem 387:135–138
377. Züchner H, Boes N (1972) Ber Bunsenges Physik Chem 76:783–790
378. Krapivnyi NG (1982) Electrokhimiya 18:1174–1178
379. Krapivnyi NG (1983) Electrokhimiya 19:36–40
380. Artman D, Flanagan TB (1973) J Phys Chem 77:2804–2807
381. Maestas S, Flanagan TB (1973) J Phys Chem 77:850–854
382. Grdeń M (2001) PhD Thesis, Warsaw University
383. Comisso N, De Ninno A, Del Giudice E, Mengoli G, Soldan P (2004) Electrochim Acta 49:1379–1388
384. Opara L, Klein B, Züchner H (1997) J Alloy Comp 253–253:378–380
385. Barlag H, Opara L, Züchner H (2002) J Alloy Comp 330–332:434–437
386. Beden B, Lamy C, de Tacconi NR, Arvia AJ (1990) Electrochim Acta 35:691–704
387. Conway BE, Angerstein-Kozlowska H, Sharp WBA, Criddle EE (1973) Anal Chem 45:1331–1336
388. Qian SY, Conway BE, Jerkiewicz G (2000) Int J Hydrogen Energy 25:539–550
389. Conway BE, Barber JH, Gao L, Qian SY (1997) J Alloys Compd 253–254:475–480
390. Muralidharan S, Kulandainathan A, Kapali V (1994) Int J Hydrogen Energy 19:219–222
391. Leiva EPM, Santos E, Iwasita T (1986) J Electroanal Chem 215:357–367
392. Couto A, Rincón A, Pérez MC, Guttiérrez C (2001) Electrochim Acta 46:1285–1296
393. Breiter MW (1984) J Electroanal Chem 180:25–29
394. Czerwiński A, Sobkowski J, Więckowski A (1974) Int J Appl Radiat Isot 25:295–300
395. Łukaszewski M, Czerwiński A (2007) J Electroanal Chem 609:54
396. Ibl N, Gut G, Weber M (1973) Electrochim Acta 18:307–314
397. Leger J-M (2005) Electrochim Acta 50:3123–3129
398. Rousset JL, Bertolini JC, Miegge P (1996) Phys Rev B 53:4947–4957
399. Ruban AV, Skriver HL, Nørskov JK (1999) Phys Rev B 59:15990–16000

400. Løvvik OM, Opalka SM (2008) Surf Sci 602:2840–2844
401. Noh H, Clewley JD, Flanagan TB, Craft AP (1996) J Alloys Comp 240:235–248
402. Tsionsky V, Daikhin L, Urbakh M, Gileadi E (2004) In: Bard AJ, Rubinstein I (eds) Electroanalytical chemistry. A series of advances, vol 22. Marcel Dekker, New York, pp 2–99
403. Hepel M (1999) In: Wieckowski A (ed) Interfacial electrochemistry. Marcel Dekker, New York, pp 599–630
404. Buttry DA, Ward MD (1992) Chem Rev 92:1355–1379
405. Buttry DA (1991) In: Bard AJ (ed) Electroanalytical chemistry. Aseries of advances, vol 17. Marcel Dekker, New York, pp 1–83
406. Schumacher R (1990) Angew Chem Int Ed Engl 29:329–343
407. Deakin MR, Buttry DA (1989) Anal Chem 61:1147A–1154A
408. Thompson M, Kipling AL, Duncan-Hewitt WC, Rajaković L, Čavić-Vlasak BA (1991) Analyst 116:881–890
409. EerNisse EP (1972) J Appl Phys 43:1330–1337
410. EerNisse EP (1973) J Appl Phys 44:4482–4485
411. Sauerbrey G (1959) Z Phys 155:206–222
412. Grdeń M (2009) Electrochim Acta 54:909–920
413. Grdeń M, Czerwiński A (2008) J Solid State Electrochem 12:375–385
414. Huggins RA (2000) Solid State Ionics 134:179–195
415. Frąckowiak E, Béguin F (2001) Carbon 39:937–950
416. Conway BE (1991) J Electrochem Soc 138:1539–1548
417. Sarangapani S, Tilak BV, Chen C-P (1996) J Electrochem Soc 143:3791–3799
418. Zhang Y, Feng H, Wu X, Wang L, Zhang A, Xia T, Dong H, Li X, Zhang L (2009) Int J Hydrogen Energy 34:4889–4899
419. Obreja VVN (2008) Physica E 40:2596–2605
420. Wang J (1981) Electrochim Acta 26:1721–1726
421. Friedrich JM, Ponce-de-León C, Reade GW, Walsh FC (2004) J Electroanal Chem 561:203–217
422. Rogulski Z, Lewdorowicz W, Tokarz W, Czerwiński A (2004) Pol J Chem 78:1357–1370
423. Czerwiński A, Dmochowska M, Grdeń M, Kopczyk M, Wójcik G, Młynarek G, Kołata J, Skowroński JM (1999) J Power Sources 77:28–33
424. Czerwiński A, Żelazowska M (1996) J Electroanal Chem 410:55–60
425. Czerwiński A, Żelazowska M (1997) J Power Sources 64:29–34
426. Rogulski Z, Czerwiński A (2003) J Power Sources 114:176–179
427. Rogulski Z, Czerwiński A (2003) J Solid State Electrochem 7:118–121
428. Rogulski Z, Chotkowski M, Czerwiński A (2006) J New Mat Elect Syst 9:333–338
429. Rogulski Z, Chotkowski M, Czerwiński A (2006) J New Mat Elect Syst 9:3401–3408
430. Czerwiński A, Obrębowski S, Kotowski J, Rogulski Z, Skowroński JM, Krawczyk P, Rozmanowski T, Bajsert, Przystałowski M, Buczkowska-Biniecka M, Jankowska E, Baraniak M (2010) J Power Sources 195:7524–7529
431. Czerwiński A, Obrębowski S, Kotowski J, Rogulski Z, Skowroński JM, Bajsert M, Przystałowski M, Buczkowska-Biniecka M, Jankowska E, Baraniak M, Rotnicki J, Kopczyk M (2010) J Power Sources 195:7530–7534
432. Pell WG, Conway BE (1996) J Power Sources 63:255–266
433. Piela P, Rogulski Z, Krebs M, Pytlik, Schmalz M, Dłubak J, Karwowska M, Gumkowska A, Czerwiński A (2010) J Electrochem Soc 157:A254–A258
434. Rogulski Z, Dłubak J, Karwowska M, Krebs M, Pytlik E, Schmalz M, Gumkowska A, Czerwiński A (2009) J Power Sources 195:7517–7523